ARIZONA STATE UNIVERSITY

Relaxation Models for Self-Regulated Coarse-Graining: Application to Generalized Langevin Equations and Brownian Motion

by

Eron Ristich

A thesis submitted in partial fulfillment for the
degree of Bachelors of Science, with Honors

in the
Ira A. Fulton Schools of Engineering
Yoshihiro Kobayashi

April 2024

"If I have seen further it is by standing on the shoulders of giants."

Isaac Newton

ARIZONA STATE UNIVERSITY

Abstract

Relaxation Models for Self-Regulated Coarse-Graining: Application to Generalized Langevin Equations and Brownian Motion

by Eron Ristich

The timescale of a simulation, determined by its size of time step, is an incredibly important consideration for resolving quickly varying dynamics. Indeed, if one chooses an observation timescale larger than the fastest forces in a dynamical system, the intricate details produced by that force's fluctuations are lost. As such, for large time steps, we require integrators that are capable of capturing the effect of these missed forces, perhaps in a statistical sense if not exactly. This problem is difficult to solve in general. As such, for simulations where these high frequency details do not need to be resolved, lower order models must be employed that resolve the overall effect of these high frequency details by construction. A representative example of this is the modeling of molecular dynamics and Brownian motion. High order models of Brownian motion, such as the generalized Langevin equations, are computationally infeasible when one wants to resolve the dynamics of, for example, a pollen particle in water. A more reasonable choice of model might be the Langevin equations or even further, the overdamped Langevin equations. As a case study, by posing the generalized Langevin equations as a relaxation system, we show how in choosing the size of time step, we automatically reduce to the effective model, without ever explicitly choosing the model used.

Acknowledgements

I'd like to thank my thesis director Professor Yoshihiro Kobayashi, and committee member Dr. Sean Seyler, for their continual help and support throughout the year of work that went into this thesis, and for many meaningful conversations during that time.

I would also like to thank my family for their unwavering love and motivation; my father for countless phone calls, my mother for unconditional support, and my brother for always helping out.

Thank you all.

Contents

List of Figures

List of Tables

Symbols

$\mathbf{x}$	position	m
$\mathbf{v}$	velocity	m/s
$\mathbf{s}$	auxiliary variable	m/s
$\mathbf{f}(t)$	deterministic force term	N
T	temperature	K
γ	Stokes friction coefficient	1/s
ω	kernel constant	dimensionless
ν	kernel constant	dimensionless
$\boldsymbol{\xi}$	random variable	various
$\boldsymbol{\mathcal{N}}$	standard normal random variable	various
k_B	Boltzmann constant	1.3806 J/K

Chapter 1

Introduction

The classical mathematical model of diffusion, Brownian motion, is a popular set of equations representing the path of a particle as a random walk within a fluid domain. However, the introduction of a random variable to equations of motion came with a disclaimer that there exist actions that occur on too high of a frequency to feasibly resolve. To what extent are important dynamical properties smoothed over when we make this simplifying assumption? What kind of information can we recover using these limited models?

1.1 Brownian Motion

In the case of so-called Brownian dynamics, we can physically think of this randomness as a consequence of the particle's high collision frequency with other particles that effectively randomizes the Brownian particle's velocity after each collision. This, in particular, handles the case of a large particle moving among many smaller ones, called bath or solvent particles. One can imagine how such a particle might experience countless small impulses that effectively randomize its motion. Consequently, Brownian motion is often referred to as – and simulated as – a random walk. For example, figure 1.1a shows a blown up example of a large particle surrounded by bath particles and travelling in two dimensions that is undergoing velocity randomization due to the numerous collisions with the bath particles. Figure 1.1b then shows how the trajectory of the tagged particle might look if we observed it for a considerable amount of time.

Although the motion of these particles are random and their individual trajectories are not necessarily useful, the mean behavior of many particle trajectories provides insight into the macroscopic behavior of fluids. Indeed, as time increases, a dense collection of particles will tend to spread evenly throughout the bath. This process is a precursor to a concept called diffusion, which describes the general tendency of particle density heading towards equilibrium across

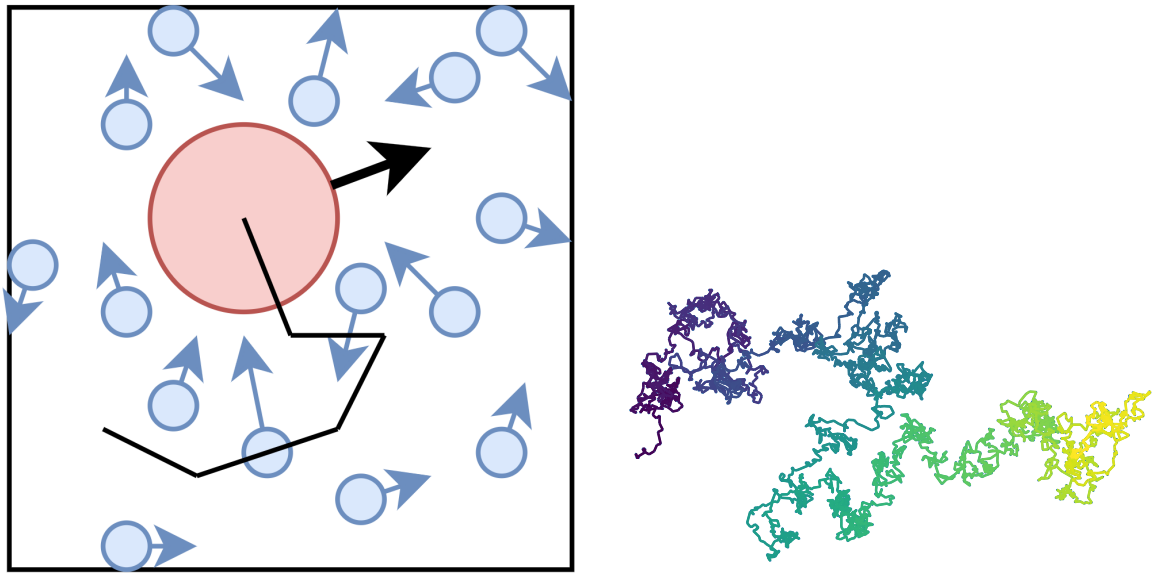

(A) A particle undergoing Brownian motion, such as a pollen particle in water. Here, the large red particle is jostled by many smaller bath particles

(B) Dense sampling of the path of a particle undergoing 2D Brownian motion

FIGURE 1.1: Examples of Brownian motion

space. For example, diffusion is a critical process for biological systems, and is a fundamental transport mechanism for macromolecules in cells [1].

1.2 Langevin Dynamics

Such a model is acceptable when inertial effects are negligible, as a particle with little mass is more prone to abrupt changes in momentum due to the perturbations induced by the bath particle. For a heavy particle, a more general model, known as Langevin dynamics, provides a more accurate description of the motion. The physical interpretation of these equations reduces to a drag force preserving inertia, and a random force that statistically models the collective result of collisions with the solvent particles of the bath. For example, figure 1.2a shows a blown up example of a large and heavy particle surrounded by several bath particles. Despite the numerous perturbations applied to this heavy particle, its direction of motion is relatively unchanged. Similarly, at short time scales, particles evolving under Langevin dynamics tend to maintain their direction due to their inertia. Figure 1.2b then shows how the trajectory of the tagged particle might look if we observed it for a considerable amount of time. In particular, compared to figure 1.1b, the particle undergoing Langevin dynamics visibly appears to have a more continuous path, which is a consequence of its inertia.

One might imagine, however, that if the drag force were high enough, a particle's velocity would be solely determined by the random fluctuations imparted to it by the bath. Indeed, this

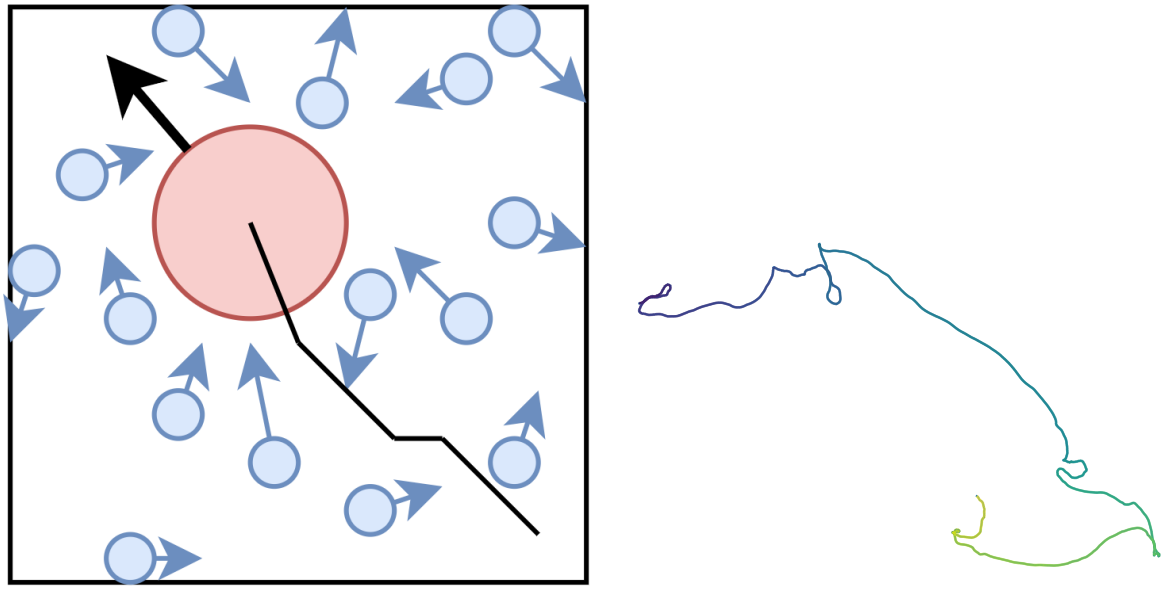

(A) A particle undergoing Langevin dynamics, which largely tends to preserve its inertia despite many small perturbations due to the bath particles

(B) Dense sampling of the path of a particle undergoing underdamped Langevin dynamics

FIGURE 1.2: Examples of Langevin dynamics

is the case; when Langevin dynamics are overdamped, the model reduces to that of Brownian motion. This kind of relaxation can actually occur in another way. If our observation time scale – the frequency at which we observe the state of a tagged particle – is large, our observations might demonstrate that a particle almost instantly relaxes to the equilibrium solution, and as such, appears to have the form of a random walk.

1.3 Generalized Langevin Dynamics

When the characteristic time scale of collisions between a tagged particle and the bath particles become similar – i.e. the rates at which particles collide with each other and the rate at which they collide with the tagged particle – an even higher order model is needed. Consider, for example, a particle moving in a viscoelastic fluid, which is a fluid that has viscous and elastic properties, in the sense that it resists shear flow, but also tends to return to its original form after stress is removed. This particle imparts some stress on the fluid which propagates to other bath particles before the viscoelastic response is later experienced by the tagged particle itself. This effect that is delayed in time requires a term that is a function of a particle's past velocities. As such, in generalized Langevin dynamics, an additional memory kernel is introduced which is a convolution of the past velocities of the particle, and is capable of modeling these complex reactionary effects from the bath.

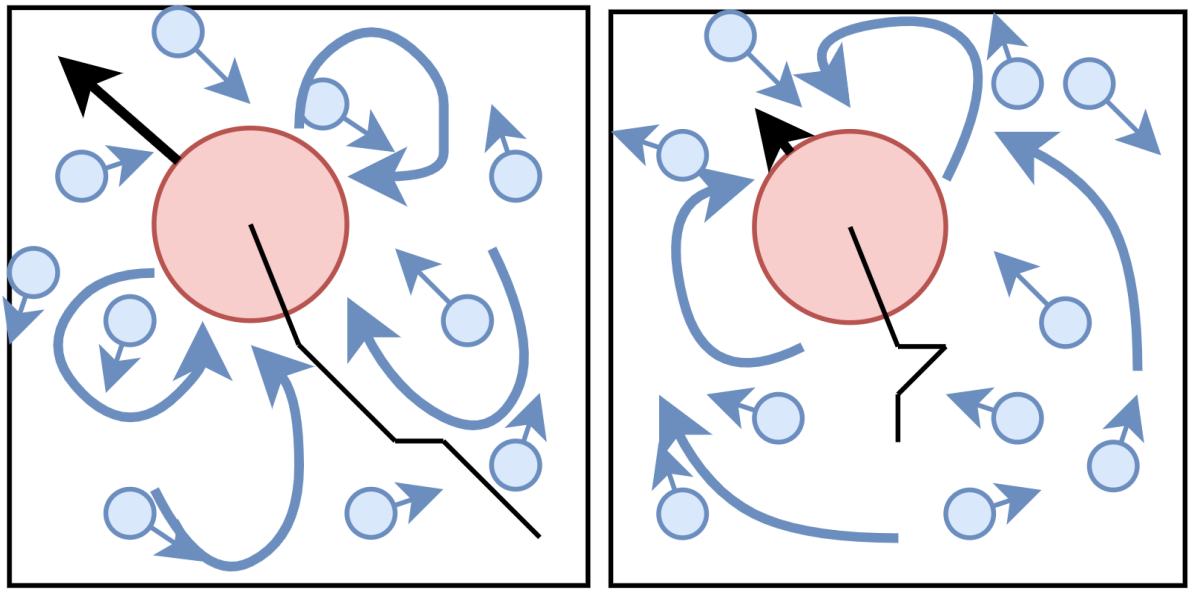

(A) A particle undergoing superdiffusive generalized Langevin dynamics, where thick blue lines represent the time delayed response of the bath, boosting the motion of the particle

(B) A particle undergoing subdiffusive generalized Langevin dynamics, where thick blue lines represent the time delayed response of the bath, acting as a drag force

FIGURE 1.3: Examples of generalized Langevin dynamics

Visually, the trajectories of such a particle are often somewhat indistinguishable from the trajectory of a standard Langevin particle. Further, the form of the particle trajectories are heavily dependent on the type of memory kernel, which may function to provide boosts to the particle's velocity (superdiffusive), or serve as an additional drag force (subdiffusive). Figure 1.3a shows an example of a particle that moves due to superdiffusive generalized Langevin dynamics, where the viscous response of the bath due to the particle's past motion causes a stress in the direction of motion, effectively boosting the tagged particle's velocity. Figure 1.3b shows an example of a particle that moves due to subdiffusive generalized Langevin dynamics, where the elastic response of the bath due to the particle's past motion causes a stress counter to the direction of motion, effectively acting as a drag force to the tagged particle's velocity.

Many researchers have developed numerical integration schemes for the GLE, each of which handle the integration of the memory kernel slightly differently. Traditionally, handling the memory kernel term requires storing a moving history of particle velocities and numerically integrating over them, or storing sequences of random numbers to handle the random force with non-trivial correlations in time [2–4]. Often, this leads to large memory requirements or computational expense.

For memory kernels in the form of a power-law [5], it has been recently shown that the generalized Langevin equations can be numerically integrated in a computationally and spatially efficient way [6, 7]. However, these algorithms, as we will show, have errors that grow as the size of time step grows.

1.4 Self-regulated Coarse-graining

All these models of Brownian motions model the same macroscopic behavior in the sense that their long time behavior recovers certain properties of the particle's motion, such as the long time diffusion coefficient. Indeed, higher order models such as Langevin dynamics or generalized Langevin dynamics improve the descriptions of the particle trajectories at fast time scales. However, a sparse sampling in time of these trajectories effectively steps over the fast time scale dynamics resolved by these higher order models, and effectively removes the need to have resolved those fast time scales in the first place. We take advantage of this fact to allow the time step to choose the effective model. Simply, as the time step grows, our algorithm no longer resolves fast time scale dynamics, and instead steps over them in a statistical sense as a lower order model might do. As such, in this thesis, we construct a novel self-regulating algorithm for Brownian motions whose mathematical formulation reduces, as a function of time step, from generalized Langevin dynamics to Langevin dynamics and finally to overdamped Brownian motion, all while preserving the correct diffusion coefficient and only resolving the appropriate time scales.

In chapter 2, we provide relevant background information about the generalized Langevin equations, and derive an extended Markovian embedding of the equations using a Prony series. In chapter 3 we compare and derive popular alternative integrators for the GLE, propose our integrator, and derive an expression for the time step rescaling parameter. In chapter 4, we conduct an analytical error analysis and numerically evaluate our integrator in the zero potential case and in a harmonic oscillator potential, comparing our method with other popular integrators. Our findings and directions for future work are summarized in chapter 5.

Chapter 2

Background and Theory

In classical physics, dynamics of a system are described by Newton's 2nd law of motion, which describe the motion of particles as a function of their mutual and external interactions. Such systems often involve a large number of particles, which makes obtaining a brute-force solution of these classical equations analytically and computationally intractable. A such, it is common to perform a dimensionality reduction to obtain models that yield tractable analysis, often referred to as a coarse-graining. Many popular equations of motion are found in physics and chemistry, including continuum models such as the Navier-Stokes equations, kinetic rate equations for chemical reactions, or the equations of equilibrium thermodynamics. Indeed, Brownian motion and Langevin dynamics are also coarse-grained models which model the motion of a particle immersed in a fluid. The generalized Langevin equation, while still a coarse-grained model, can actually be used as the basis for a quite general, versatile, and robust description of complex systems in physics and chemistry.

While there is no general means by which one can identify an optimal coarse-grained model for a classical system, many powerful methods have been developed to construct these coarse-grained methods in a principled manner. One such method is the Mori-Zwanzig projection operator technique, which, roughly speaking, involves projecting the full dynamical coordinates of a system onto a subset of degrees of freedom of interest and gathering the remaining degrees of freedom into a compact statistical description that takes the form of a stochastic force [8, 9]. In this way, the projection operator technique can be used to produce the generalized Langevin equations, where the degrees of freedom of interest are the position and velocity of a tagged particle, and the remaining degrees of freedom belong to the bath. Notably, the degrees of freedom of interest do not have to be grouped in this way, and could be collective coordinates of many particles, or a vector field of such particles, thus providing a hydrodynamic description.

For simplicity, however, we will discuss generalized Langevin dynamics primarily in the context of a single particle immersed in a potentially complex fluid. In this representation,

the trajectory of a single particle can be described by a memory kernel that accommodates for Stokes drag and complex , a slowly varying external force term determined by the underlying potential of the system, and a quickly varying stochastic force term that describes the dynamics of the bath.

2.1 Background of Stochastic Dynamics Integrators

Classical algorithms for molecular dynamics simulations evaluate Newtonian dynamics using general-purpose integrators such as position Verlet or Runge-Kutta, which are generally computationally efficient as they require a minimal number of force evaluations per time step. However, such integrators are limited by the conditions of the systematic force term. For stochastic equations of motion, the random force term constrains the time step by its velocity relaxation time γ^{-1} [10], which is often a heavily restrictive condition, especially for systems that have otherwise slowly varying potentials.

In 1982 and 1988, Van Gunsteren and Berendsen introduced two third-order integrators for stochastic dynamics which lifted the restriction on time step to only that of the systematic force term [10, 11]. Their work was motivated by existing third-order general integration methods, position Verlet and leap-frog, to which their algorithms reduce to in the no-friction limit, $\gamma = 0$. In particular they are able to lift this restriction by explicitly integrating the random force term, splitting the force updates into a deterministic force update and a stochastic force update.

Integration of the generalized Langevin equations is more difficult, in part due to the convolution integral for the drag term, requiring precise information about past velocities of the system. To accomodate for that, in 1989, Smith and Harris proposed a numerical integrator for the generalized Langevin equations that models the memory kernel as an autoregressive stochastic recurrence relation, depending linearly on its previous values and a stochastic term [2].

However, an even more complicated consequence of the memory kernel is the complex correlations in time introduced by the stochastic term, which must necessarily satisfy the same kernel over which the velocities are convolved. In 2013, Baczewski and Bond introduced an extended variable formalism of the generalized Langevin equations that uses a positive Prony series to deconstruct the memory kernel and the stochastic term into a discrete set of auxiliary variables, which by construction satisfy the fluctation-dissipation relation. Their work has been implemented into the LAMMPS code, which is an open source code for molecular dynamics simulations.

2.2 Relaxation Systems

Many physical systems, with perturbations of arbitrary size, will eventually, given enough time, return to some equilibrium state, which is often independent of the initial perturbation. For example, a damped harmonic oscillator will, over time, return to its equilibrium position. For physical systems with known asymptotic behavior, we can guarantee that any integrator for the system recovers that behavior. The primary concern is the extent of this correction. How can we use a relaxation method to recover the correct asymptotic behavior while preserving the dynamics?

2.2.1 Deterministic Relaxation Systems

As a motivating example, consider a particle with a simple linear drag force

$$\dot{x} = v(t) \tag{2.1a}$$

$$\dot{v} = -\gamma v(t) + \frac{1}{m} f(t) \tag{2.1b}$$

For general integrators, there are time step restrictions introduced both due to the drag term, $-\gamma v(t)$, and the force term, $\frac{1}{m} f(t)$. Note that this is in the form of a relaxation system, as after some perturbation the drag term tends to pull the particle towards 0 velocity over time.

In particular, in the overdamped regime where inertial effects are near negligible, the equations of this particle reduce to

$$\dot{x} = \frac{1}{\gamma m} f(t) \tag{2.2}$$

Typically, this form arises in the zero-mass or inertialess limit, having $m\dot{v} = 0$ [12], where we substitute a rescaled friction coefficient $\zeta = \gamma m$. Alternatively, if we consider the limit where γt is large, we recover the same overdamped dynamics. The exact solution of velocity has

$$\dot{x} = v(t) = v(0)e^{-\gamma t} + \frac{1}{\gamma m} f(t) \tag{2.3}$$

which, in the limit of γt large has the same form as 2.2. We show that this limit can be recovered by an implicit integrator such as the backward Euler method by allowing the time step to grow such that $\gamma \Delta t$ is large.

In backward Euler, we integrate equations 2.1a and 2.1b as

$$v^{n+1} = v^n - \gamma \Delta t v^{n+1} + \frac{\Delta t}{m} f(t) \tag{2.4a}$$

$$x^{n+1} = x^n + \Delta t v^{n+1} \tag{2.4b}$$

which gives us an expression for v^{n+1} as

$$v^{n+1} = \frac{v^n + \frac{\Delta t}{m} f(t)}{1 + \gamma \Delta t} \tag{2.5}$$

In the limit as Δt grows large and under the assumption that $f(t)$ is slowly varying, this reduces to

$$v^{n+1} \approx \frac{f(t)}{\gamma m} \tag{2.6}$$

which exactly corresponds to the overdamped equations.

2.2.2 Stochastic Relaxation Systems

For a stochastic relaxation system, simply taking a large Δt does not recover the overdamped limit. Consider a particle whose dynamics are governed by the Langevin equation

$$\dot{x} = v(t) \tag{2.7a}$$

$$\dot{v} = -\gamma v + \frac{1}{m} f(t) + \sqrt{\frac{2\gamma k_B T}{m}} W(t) \tag{2.7b}$$

where W is a white noise term called a Wiener process with 0 mean and units of time$^{-1/2}$, satisfying $\langle W(t) W(t') \rangle = \delta(t - t')$.

The overdamped limit of this set of equations, obtained again in the zero-mass or inertialess limit, is

$$\dot{x} = \frac{1}{\gamma m} f(t) + \sqrt{\frac{2 k_B T}{\gamma m}} W(t) \tag{2.8}$$

which corresponds to Brownian motion, where we can write the friction coefficient as $\zeta = \gamma m$.

If we consider a backward Euler-Maruyama integrator, we integrate equations 2.7a and 2.7b as

$$v^{n+1} = v^n - \gamma \Delta t v^{n+1} + \frac{\Delta t}{m} f(t) + \sqrt{\frac{2\gamma k_B T \Delta t}{m}} \mathcal{N}(t) \tag{2.9a}$$

$$x^{n+1} = x^n + \Delta t v^{n+1} \tag{2.9b}$$

where we note the $\sqrt{\Delta t}$ term in the random variable arises because $\Delta \mathcal{N}^n = \mathcal{N}^{n+1} - \mathcal{N}^n$ is a Gaussian random variable with zero mean and Δt variance [13]. See the description of Wiener processes in appendix A. This gives us an expression for v^{n+1} as

$$v^{n+1} = \frac{v^n + \frac{\Delta t}{m} f(t) + \sqrt{\frac{2\gamma k_B T \Delta t}{m}} \mathcal{N}(t)}{1 + \gamma \Delta t} \tag{2.10}$$

In the limit as Δt grows large and under the assumption that $f(t)$ is slowly varying, this reduces to

$$v^{n+1} \approx \frac{1}{\gamma m} f(t) + \sqrt{\frac{2k_B T}{\gamma m \Delta t}} \mathcal{N}(t) \approx \frac{1}{\gamma m} f(t) \tag{2.11}$$

Here, the random variable under an update with large Δt has 0 variance, quite unlike the corresponding overdamped equation. Further, a naïve rescaling of the random variable with a constant $\sqrt{\Delta t}$ produces the incorrect short-time dynamics, despite having the correct overdamped behavior. A well motivated correction arises from realizing that $-\gamma v + \xi$ is an exactly solvable Ornstein-Uhlenbeck process, where ξ is the random force term. As shown by [14], there exists a time step rescaling parameter for the deterministic force updates that allows for the correct short-time dynamics while preserving the long-time statistics of the Langevin equations.

2.2.3 Rescaling Parameter for the Langevin Equations

In this section, we provide a brief overview of the work done by [14] to show how the introduction of a time step rescaling parameter allows the diffusion coefficient – and other dynamical variables – to be correctly resolved for arbitrarily large time steps.

The Langevin equation can be written as

$$\dot{x} = v \tag{2.12a}$$

$$\dot{v} = \frac{f(t)}{m} - \gamma v + \sqrt{\frac{2\gamma k_B T}{m}} \eta(t) \tag{2.12b}$$

where γ is a friction coefficient or collision frequency, f is some slowly – with respect to the collision frequency – varying external force on the system, and η is a white noise process. The authors choose a set of long-time desiderata from literature that their integrator must recover, including the diffusion coefficient in zero-force and the mean squared velocity (i.e., the Maxwell Boltzmann distribution). For an in depth discussion of these useful discrete-time integrator properties, we refer the reader to [15].

In particular, by requiring the zero-force diffusion coefficient, Sivak et. al find that a simple time step rescaling parameter applied to the deterministic updates of position and velocity allows their family of integrators to recover nearly all of the desiderata they describe.

Their integrator can be described succinctly in the form of a stochastic Leapfrog integrator

$$v\left(n + \frac{1}{2}\right) = \theta v\left(n - \frac{1}{2}\right) + (1 + \theta)\frac{b\Delta t}{2}\frac{f(n)}{m} + \sqrt{(1 - \theta^2)\frac{k_B T}{m}}\mathcal{N} \tag{2.13a}$$

$$x(n+1) = x(n) + b\Delta t v\left(n + \frac{1}{2}\right) \tag{2.13b}$$

when positions and velocities at half steps can be safely ignored. Here, we have $\theta = e^{-\gamma\Delta t}$, and the time step rescaling parameter b has the form

$$b = \sqrt{\frac{2}{\gamma\Delta t}\tanh\frac{\gamma\Delta t}{2}} \tag{2.14}$$

In this form, discrete-time integration in the low friction limit $\gamma\Delta t \ll 1$ has the value of b approach 1, which, in the limit as Δt approaches 0, is the expected result for the continuous-time equations. In the high friction limit $\gamma\Delta t \gg 1$, this has the form $b = \sqrt{\frac{2}{\gamma\Delta t}}$, which, when substituted into the relaxation system described in section 2.2.2, yields a random variable with the same variance as in the overdamped regime.

2.3 The Generalized Langevin Equations

The generalized Langevin equation (GLE), which can be derived from the Mori-Zwanzig projection operator formalism [8, 9], is a stochastic dynamical model that captures the behavior of a wide range of diffusive phenomena. These equations extend the idea of Langevin dynamics, where a tagged particle experiences forces from a surrounding bath at a high frequency, which are represented in a statistical sense rather than deterministically resolved. The collective action of the collisions of bath particles with the solute can be approximated by a linear combination of deterministic and fluctuating forces, where the deterministic forces vary at a considerably lower frequency than the stochastic forces. This model is sufficient when the characteristic time scale of tagged particles is far larger than that of the solvent particles. The generalized Langevin equation arises when this assumption no longer holds, and in turn introduces a random force with non-trivial correlations with time. In this section, we review the generalized Langevin Equations, and derive a Markovian embedding form of the positive Prony series, which will then be the target for integration.

The non-Markovian form of the GLE is given by

$$\dot{\mathbf{x}} = \mathbf{v}(t) \tag{2.15}$$

$$\dot{\mathbf{v}} = \frac{1}{m}\mathbf{f}(t) - \int_0^t \hat{K}(t-t')\mathbf{v}(t')dt' + \hat{\boldsymbol{\xi}}(t) \tag{2.16}$$

where, generally, m is the mass of the particle, $\hat{K}$ is a memory kernel, and $\hat{\boldsymbol{\xi}}$ is a stationary Gaussian process satisfying the fluctuation-dissipation relation (FDR)

$$\langle\hat{\boldsymbol{\xi}}^i(0)\hat{\boldsymbol{\xi}}^j(t)\rangle = \frac{k_BT}{m}\hat{K}(t)\delta_{ij} \tag{2.17}$$

where the i and j indices represent components of the vector.

Following the work of [7] and [6], we choose a general form of the memory kernel called a positive Prony series, motivated by its wide use in literature [16], and because it can also be viewed as an approximation of a power law [17], which has seen extensive use in the past [18, 19]. The memory kernel takes the form of

$$\hat{K}(t) = \sum_{k=1}^{M} \omega_k^2 e^{-\nu_k t} \tag{2.18}$$

where M is a non-negative integer corresponding to the number of modes, $\omega_k = \frac{\tilde{\omega_k}}{\sqrt{\epsilon}}$, and $\nu_k = \frac{\tilde{\nu_k}}{\epsilon}$, having ϵ be a rescaling factor and ω_k and ν_k being two constant parameters.

We can define auxiliary variables to capture the kth mode in the Prony series

$$\mathbf{z}_k = -\int_0^t \omega_k e^{-\nu(t-t')} \mathbf{v}(t') dt' \tag{2.19}$$

Differentiating the result gives

$$\dot{\mathbf{z}}_k = -\nu_k \mathbf{z}(t) - \omega_k \mathbf{v}(t) \tag{2.20}$$

We then construct a random force for each mode that satisfies FDT and has a form similar to equation 2.20. Consider the random variables

$$\dot{\boldsymbol{\xi}}_k = -\nu_k \boldsymbol{\xi}_k(t) + \sqrt{2\nu_k \frac{k_B T}{m}} \boldsymbol{\mathcal{N}}_k(t) \tag{2.21}$$

where $\boldsymbol{\mathcal{N}}_k$ is a random variable with 0 mean and unit variance. This describes an Ornstein-Uhlenbeck process which has 0 mean and time correlation $\langle \boldsymbol{\xi}_k^i(0) \boldsymbol{\xi}_k^j(t) \rangle = \frac{k_B T}{m} e^{-\nu_k t} \delta_{ij}$ where the i and j indices represent components of the vector. See appendix A for an overview of Ornstein-Uhlenbeck processes and their exact solutions. The weighted sum of each $\boldsymbol{\xi}_k$ yields

$$\hat{\boldsymbol{\xi}}(t) = \sum_{k=1}^{M} \omega_k \boldsymbol{\xi}_k \tag{2.22}$$

Combining $\mathbf{z}_k$ and $\boldsymbol{\xi}_k$ yields a final auxiliary variable $\mathbf{s}_k = \mathbf{z}_k + \boldsymbol{\xi}_k$. Substituting this back into equation 2.15 gives an extended variable Markovian embedding of the generalized Langevin equation

$$\dot{\mathbf{x}} = \mathbf{v}(t) \tag{2.23a}$$

$$\dot{\mathbf{v}} = \frac{1}{m}\mathbf{f}(t) + \sum_{k=1}^{M} \omega_k \mathbf{s}_k(t) \tag{2.23b}$$

$$\dot{\mathbf{s}}_k = -\nu_k \mathbf{s}_k(t) - \omega_k \mathbf{v}(t) + \sqrt{2\nu_k \frac{k_B T}{m}} \boldsymbol{\mathcal{N}}_k(t) \tag{2.23c}$$

An important consideration, and indeed a motivating reason for choosing this form, is that equation 2.23 has the auxiliary variables in the form of a relaxation system, where each $\mathbf{s}_k$ relaxes on a timescale as determined by ν_k. This is a pivotal realization for the development of our algorithm, as these timescales, when stepped over, reduce the auxiliary variable to a white noise process coupled to the velocity variable, or effectively, a Langevin equation. This effect is emphasized in our numerical algorithm, described in section 3.1.5.

2.4 Relaxation to the Langevin Equations

If we solve for $\mathbf{s}_k(t)$ in equation 2.23c, and substitute into equation 2.23b, we find

$$\dot{\mathbf{v}} = \frac{1}{m}\mathbf{f}(t) - \sum_{k=1}^{M}\frac{\omega_k}{\nu_k}\dot{\mathbf{s}}_k(t) - \sum_{k=1}^{M}\frac{\omega_k^2}{\nu_k}\mathbf{v}(t) + \sqrt{\sum_{k=1}^{M} 2\frac{\omega_k^2}{\nu_k}\frac{k_B T}{m}}\boldsymbol{\mathcal{N}}_k(t) \tag{2.24}$$

In the white noise limit, as $\epsilon \to 0$ [20], we find $\frac{\omega_k}{\nu_k} = \frac{\tilde{\omega}_k\sqrt{\epsilon}}{\tilde{\nu}_k} \to 0$, and thus, $\dot{\mathbf{v}}$ reduces to the form

$$\dot{\mathbf{v}} = \frac{1}{m}\mathbf{f}(t) - \gamma\mathbf{v}(t) + \sqrt{2\gamma\frac{k_B T}{m}}\boldsymbol{\mathcal{N}}_k(t) \tag{2.25}$$

where

$$\gamma = \sum_{k=1}^{M}\frac{\omega_k^2}{\nu_k} \tag{2.26}$$

This, notably, has the exact form of the Langevin equations, having γ as a Stokes' drag coefficient, where in physical systems, Stokes' drag has a known value of $\gamma = 6\pi r\eta v$ with no-slip boundary conditions or $\gamma = 4\pi r\eta v$ with slip, having η be fluid dynamic viscosity. We would expect, then, an integrator to be able to recover Langevin dynamics within this limit.

In the non-inertial limit as γ grows, we find this reduces further to overdamped Langevin dynamics, or Brownian motion, where the inertial term becomes negligible, as the high friction effectively "resets" the velocity over very short timescales, i.e., the past velocity is "forgotten." We can think of this intuitively as the influence of the memory kernel decaying instantaneously. Refer to [21] for further analysis of this asymptotic behavior within the GLE.

This reduction of models from the GLE to the conventional Langevin equation and finally to overdamped Brownian dynamics is an example of a stochastic relaxation system, and a motivating reason behind the purpose of the time step rescaling and relaxation method. It is clear that as time step grows, for the GLE or for Langevin dynamics, a particle's velocity and position become less and less correlated with its history of velocities and positions. Indeed, if one takes a large enough time step, decaying memory effects in the GLE become almost negligible.

Regardless of friction coefficients or size of time step, an ideal integrator should be able to produce the same or similar statistics as it might in the limit as the integrator approaches the continuous-time equation of motion.

2.5 Superdiffusive GLE

In the superdiffusive case, a small change is needed to to the Markovian embedding.

$$\dot{\mathbf{x}} = \mathbf{v}(t) \tag{2.27a}$$

$$\dot{\mathbf{v}} = \frac{1}{m}\mathbf{f}(t) - \sum_{k=1}^{M} \omega_k \mathbf{s}_k(t) \tag{2.27b}$$

$$\dot{\mathbf{s}}_k = -\nu_k \mathbf{s}_k(t) - \omega_k \mathbf{v}(t) + \sqrt{2\nu_k \frac{k_B T}{m}} \boldsymbol{\mathcal{N}}_k(t) \tag{2.27c}$$

The sole modification is in equation 2.27b, where the sign before the summation has flipped. This change makes intuitive sense; particles in the bath displaced by the tagged particles motion push the particle in the same direction [22]. In the case of viscoelastics, described by the positive sign in equation 2.23b, the bath instead produces a slowly relaxing viscous force that acts against the motion of the particle [23].

Further investigation of the superdiffusive GLE is set aside for future work.

Chapter 3

Numerical Methods

There have been a variety of methods developed to integrate these equations of motions, however, recent developments have popularized the use of splitting methods for the GLE [6, 7].

In this chapter, we will go over the derivations and motivations for the current state-of-the-art algorithms, and justify the choices made in the development of our time step rescaling algorithm.

3.1 Strang Splittings

Strang splitting is a numerical method for the integration of differential equations, and is a method that has been used in the past for Langevin equations [14] and for the GLE [6, 7]. Effectively, for a differential equation that is decomposable into a sum of differential operators, we solve each operator independently, and then combine their results. See appendix B for a more in depth explanation of how Strang splitting works to obtain second order accuracy.

Because we split the differential equation into many sub-problems, there exist many different combinations of differential operators that can be solved for. We choose a specific subset of splittings here that are popular in literature, but note that other such splittings exist which could be investigated as well.

3.1.1 Position and Velocity Updates

The simplest sub-problem to solve are those corresponding to the deterministic Newtonian updates to position and velocity. If we consider the Liouvillian of the system to be $\mathcal{L}$, these first two splittings yield a splitting

$$\mathcal{L} = \mathcal{L}_x + \mathcal{L}_v + \dots \tag{3.1}$$

where $\mathcal{L}_x$ corresponds to the deterministic position update, and $\mathcal{L}_v$ corresponds to the deterministic velocity update.

	$\mathcal{L}_x$	$\mathcal{L}_v$	...
$\dot{\mathbf{x}}$	$\mathbf{v}(t)$		
$\dot{\mathbf{v}}$		$\frac{1}{m}\mathbf{f}(t)$	$\sum_{k=1}^{M} \omega_k \mathbf{s}_k(t)$
$\dot{\mathbf{s}}_k$			$-\nu_k \mathbf{s}_k(t) - \omega_k \mathbf{v}(t) + \sqrt{2\nu_k \frac{k_B T}{m}} \boldsymbol{\mathcal{N}}_k(t)$

TABLE 3.1: Components belonging to $\mathcal{L}_x$ and $\mathcal{L}_v$

These deterministic Newtonian updates have well-developed algorithms for integration, and we can choose from a variety of methods to solve these terms.

Name	Type	Method	Accuracy
Forward Euler	Explicit	$y^{n+1} = y^n + \Delta t f(t^n, y^n)$	$O(\Delta t)$
Backward Euler	Implicit	$y^{n+1} = y^n + \Delta t f(t^{n+1}, y^{n+1})$	$O(\Delta t)$
Runge-Kutta	Explicit	$y^{n+1} = y^n + \Delta t \sum_{i=1}^{s} b_i k_i$	$O(\Delta t^4)$

TABLE 3.2: Methods of deterministic updates

We could also choose to solve these subsystems in a way similar to velocity Verlet, which is an explicit symplectic integration scheme with 3rd order accuracy.

$$\mathbf{v}^{n+1/2} = \mathbf{v}^n + \frac{\Delta t}{2m}\mathbf{f}^n \tag{3.2a}$$

$$\mathbf{x}^{n+1} = \mathbf{x}^n + \mathbf{v}^{n+1/2}\Delta t \tag{3.2b}$$

$$\mathbf{v}^{n+1} = \mathbf{v}^{n+1/2} + \frac{\Delta t}{2m}\mathbf{f}^{n+1} \tag{3.2c}$$

This symmetric form of first order forward Euler updates is indicative of how one might take advantage of Strang operator splittings to obtain higher order accuracy. We can choose to split operators in this way, splitting the solution into symmetric half time step updates

$$e^{(A+B)\Delta t} = e^{A\Delta t/2} e^{B\Delta t} e^{A\Delta t/2} + O(\Delta t^3) \tag{3.3}$$

where A and B can be arbitrary selections of $\mathcal{L}_x$ or $\mathcal{L}_v$. Following this form of velocity Verlet, and motivated by similar decisions made for integrators in literature for Langevin dynamics [14] and the GLE [6, 7], we choose to evaluate the deterministic updates to position and velocity using the first order forward Euler method.

Specifically, similar to [14], we introduce a rescaling parameter b into these updates that allows for any size time step to be chosen while maintaining statistical accuracy for known

limits. The forward Euler steps with rescaling parameter for position and velocity are then

$$\mathbf{x}^{n+1} = \mathbf{x}^n + b\Delta t\mathbf{v}^n \tag{3.4a}$$

$$\mathbf{v}^{n+1} = \mathbf{v}^n + \frac{b\Delta t}{m}\mathbf{f}^n \tag{3.4b}$$

3.1.2 Velocity and Auxiliary Variable Coupling

A more complicated sub-problem is the velocity and auxiliary variable coupling, which can be split in an increasing number of ways as the number of auxiliary variables increases.

	$\mathcal{L}_e$	$\dots$
$\dot{\mathbf{v}}$	$\sum_{k=1}^{M} \omega_k \mathbf{s}_k(t)$	
$\dot{\mathbf{s}}$		$-\nu_k \mathbf{s}_k(t) - \omega_k \mathbf{v}(t) + \sqrt{2\nu_k \frac{k_B T}{m}} \boldsymbol{\mathcal{N}}_k(t)$
	$\mathcal{L}_e^k$	$\dots$
$\dot{\mathbf{v}}$	$\sum_{k=1}^{M} \omega_k \mathbf{s}_k(t)$	
$\dot{\mathbf{s}}$	$-\omega_k \mathbf{v}(t)$	$-\nu_k \mathbf{s}_k(t) + \sqrt{2\nu_k \frac{k_B T}{m}} \boldsymbol{\mathcal{N}}_k(t)$

TABLE 3.3: Possible splits of velocity and auxiliary coupling

In table 3.3, we describe two different splits, used by [6] and [7] respectively. We note that in [6], they have a single operator for the entire summation term in the velocity, while in [7], they have M operators, one for each term in the summation coupled with a corresponding term in the related auxiliary equation.

Similarly to the choices made for velocity Verlet, [6] choose to integrate $\mathcal{L}_e$ using forward Euler, producing the update

$$\mathbf{v}^{n+1} = \mathbf{v}^n + \Delta t \sum_{k=1}^{M} \omega_k \mathbf{s}_k(t) \tag{3.5}$$

For the second splitting, note that for each $\mathcal{L}_e^k$, we have the subsystem

$$\dot{\mathbf{v}} = \omega_k \mathbf{s}_k(t) \tag{3.6a}$$

$$\dot{\mathbf{s}}_k = -\omega_k \mathbf{v}(t) \tag{3.6b}$$

which corresponds to a harmonic oscillator with frequency ω_k. Given initial conditions $\mathbf{v}(0) = \mathbf{v}^n$ and $\mathbf{s}_k(0) = \mathbf{s}_k^n$, we have the exact solution

$$\mathbf{v}^{n+1} = \mathbf{v}^n \cos(\omega_k \Delta t) + \mathbf{s}_k^n \sin(\omega_k \Delta t) \tag{3.7a}$$

$$\mathbf{s}_k^{n+1} = -\mathbf{v}^n \sin(\omega_k \Delta t) + \mathbf{s}_k^n \cos(\omega_k \Delta t) \tag{3.7b}$$

Motivated by this exact solution, if we consider a similar split as [7] but grouped into a single operator, as described in table 3.4, we can solve the entire subsystem exactly, without a need to split the coupling into multiple auxiliary Liouvillians.

	$\mathcal{L}_e$	...
$\dot{\mathbf{v}}$	$\sum_{k=1}^{M} \omega_k \mathbf{s}_k(t)$	
$\dot{\mathbf{s}}$	$-\omega_k \mathbf{v}(t)$	$-\nu_k \mathbf{s}_k(t) + \sqrt{2\nu_k \frac{k_B T}{m}} \boldsymbol{\mathcal{N}}_k(t)$

TABLE 3.4: Alternative splitting for velocity and auxiliary coupling

Now that we consider the entire summation in its entirety, we see that the velocity equation is a sum of coupled harmonic oscillators with the remaining auxiliary variable terms. We can guess that an exact solution to this differential equation might take a similar form as the solution to the harmonic oscillator

$$\mathbf{v}(t) = A\cos(ct) + B\sin(ct) + C \tag{3.8a}$$

$$\mathbf{s}_k(t) = A_k\cos(ct) + B_k\sin(ct) + C_k \tag{3.8b}$$

If we substitute this form, and solve for the coefficients, we find the exact solution of this equation with initial conditions $\mathbf{v}(0) = \mathbf{v}^n$ and $\mathbf{s}_k(0) = \mathbf{s}_k^n$ to be

$$\mathbf{v}^{n+1} = \mathbf{v}^n\cos(\omega\Delta t) + \mathbf{s}^n\sin(\omega\Delta t) \tag{3.9a}$$

$$\mathbf{s}_k^{n+1} = \mathbf{s}_k^n + \frac{\omega_k \mathbf{s}^n}{\omega}\left[\cos(\omega\Delta t) - 1\right] - \frac{\omega_k \mathbf{v}^n}{\omega}\sin(\omega\Delta t) \tag{3.9b}$$

where $\omega^2 = \sum_{k=1}^{M} \omega_k^2$ and $\mathbf{s}^n = \sum_{k=1}^{M} \omega_k \mathbf{s}_k^n/\omega$.

We choose this third form for our integrator, as it removes the need to investigate the ordering of each $\mathcal{L}_e^k$ (as each operator does not commute), and, as we describe in section 4.1, yields a well behaved rescaling parameter.

3.1.3 Auxiliary Update

Depending on the splitting chosen for the velocity and auxiliary variable coupling, the final splitting necessary corresponds to the differential operator representing the remainder of the auxiliary equation.

Table 3.5 describes the splits used by [6] and [7] respectively. As described in section 2.3, these equations correspond to Ornstein-Uhlenbeck processes, which have analytically known exact solutions.

	$\mathcal{L}_o$
$\dot{\mathbf{s}}$	$-\nu_k \mathbf{s}_k(t) - \omega_k \mathbf{v}(t) + \sqrt{2\nu_k \frac{k_B T}{m}} \boldsymbol{\mathcal{N}}_k(t)$

	$\mathcal{L}_o$
$\dot{\mathbf{s}}$	$-\nu_k \mathbf{s}_k(t) + \sqrt{2\nu_k \frac{k_B T}{m}} \boldsymbol{\mathcal{N}}_k(t)$

TABLE 3.5: Liouvillians for the auxiliary update

The first splitting, with the additional velocity term, as is done by Baczewski and Bond [6], can be solved exactly as

$$\mathbf{s}_k^{n+1} = \theta_k \mathbf{s}_k^n - (1-\theta_k)\frac{\omega_k}{\nu_k}\mathbf{v}^n + \sqrt{(1-\theta_k^2)\frac{k_B T}{m}}\boldsymbol{\mathcal{N}}_k^n \tag{3.10}$$

where $\boldsymbol{\mathcal{N}}_k^n$ is a vector of independent standard normal random variables, and $\theta_k = e^{-\nu_k \Delta t}$. Note that 3.10 involves two characteristic timescales: θ_k and ν_k, both of which appear in the term that couples the bath variable to the velocity $\mathbf{v}^n$. The disadvantage of this form is that it is not immediately clear how to obtain a closed-form expression for the timestep-rescaling parameter by solving the recurrence relations for large n. Further, the exact Ornstein-Uhlenbeck solution with drift used in this formulation approximates $\mathbf{v}^n$ as a constant, which is only the case when $\mathbf{v}^n$ is slowly varying with respect to the size of time step, which heavily restricts the maximum allowable size of time step.

The second splitting, as is done in [7, 14], can be solved exactly as

$$\mathbf{s}_k^{n+1} = \theta_k \mathbf{s}_k^n + \sqrt{(1-\theta_k^2)\frac{k_B T}{m}}\boldsymbol{\mathcal{N}}_k^n \tag{3.11}$$

where $\boldsymbol{\mathcal{N}}_k^n$ is a vector of independent standard normal random variables, and $\theta_k = e^{-\nu_k \Delta t}$.

As in our choice of splitting for the coupling term we do not have the additional velocity term, we choose this second method to solve the Ornstein-Uhlenbeck process exactly.

3.1.4 Ordering of Splittings

As described briefly in section 3.1.1, we can choose various splittings as permutations of our operators. As is done in literature, we have split our Liouvillian into

$$\mathcal{L} = \mathcal{L}_x + \mathcal{L}_v + \mathcal{L}_e + \mathcal{L}_o \tag{3.12}$$

Depending on the problem, we can add an additional operator $\mathcal{L}_h$ to describe the time evolution of the system Hamiltonian as well, having $e^{\mathcal{L}_h \Delta t}\mathcal{H}(n) = \mathcal{H}(n+1)$.

If we approximate dynamics using these Strang splittings, we have

$$e^{(A+B+C+D)\Delta t} = e^{A\Delta t/2}e^{B\Delta t/2}e^{C\Delta t/2}e^{D\Delta t}e^{C\Delta t/2}e^{B\Delta t/2}e^{A\Delta t/2} + O(\Delta t^3) \tag{3.13}$$

where (A, B, C, D) is some permutation of $(\mathcal{L}_x, \mathcal{L}_v, \mathcal{L}_e, \mathcal{L}_o)$. [6] and [7] choose the ordering $(\mathcal{L}_v, \mathcal{L}_x, \mathcal{L}_e, \mathcal{L}_o)$, and are differentiated by their choice of split, as described in section 3.1.2 and 3.1.3. Notably, this choice reduces to the standard velocity Verlet algorithm, in the absence of noise.

Motivated by this, we choose the ordering $(\mathcal{L}_v, \mathcal{L}_x, \mathcal{L}_e, \mathcal{L}_o)$, which yields a well behaved time step rescaling parameter as described in section 3.2. Empirically, other orderings may yield rescaling parameters with vertical asymptotes, which leads to numerical instabilities. Additionally, it yields a form similar to [7] and [6] which supports comparison between the three. Further, it only requires one force evaluation per step, where the force must be sampled at half steps in the integrator.

Theoretically, any permutation could be chosen and investigated, which may yield different forms of the time step rescaling parameter. The investigation of these various splittings, however, is left to future work.

3.1.5 Full Integrator

Substep	BACSCAB [6]	BAEOEAB [7]	HOURS
Position	$x^{n+1} = x^n + \Delta t v^n$	$x^{n+1} = x^n + \Delta t v^n$	$x^{n+1} = x^n + b\Delta t v^n$
Deterministic Velocity	$v^{n+1} = v^n + \frac{\Delta t}{m} f(t)$	$v^{n+1} = v^n + \frac{\Delta t}{m} f(t)$	$v^{n+1} = v^n + \frac{b\Delta t}{m} f(t)$
Velocity coupling	$v^{n+1} = v^n + \Delta t \sum_{k=1}^{M} \omega_k s^n$	Repeated sequential applications over all k, $v^{n+1} = \cos(\omega_k \Delta t) v^n + \sin(\omega_k \Delta t)$	$v^{n+1} = \cos(\omega \Delta t) v^n + s^n \sin(\omega \Delta t)$
Auxiliary coupling	N/A	$s_k^{n+1} = s_k^n \cos(\omega_k \Delta t) - v^n \sin(\omega_k \Delta t)$	$s_k^{n+1} = s_k^n + \frac{\omega_k}{\omega} s^n (\cos(\omega \Delta t) - 1) - \frac{\omega_k}{\omega} v^n \sin(\omega \Delta t)$
Ornstein-Uhlenbeck update	$s_k^{n+1} = \theta_k s_k^n - (1-\theta_k)\frac{\omega}{\nu} v^n + \xi_k$	$s_k^{n+1} = \theta_k s_k^n + \xi_k$	$s_k^{n+1} = \theta_k s_k^n + \xi_k$

TABLE 3.6: Summary of splittings chosen by different integrators in literature

In table 3.6, we summarize the updates for each integrator side by side. Here, the table and the indices does not suggest any particular ordering of these updates. Indeed, all updates

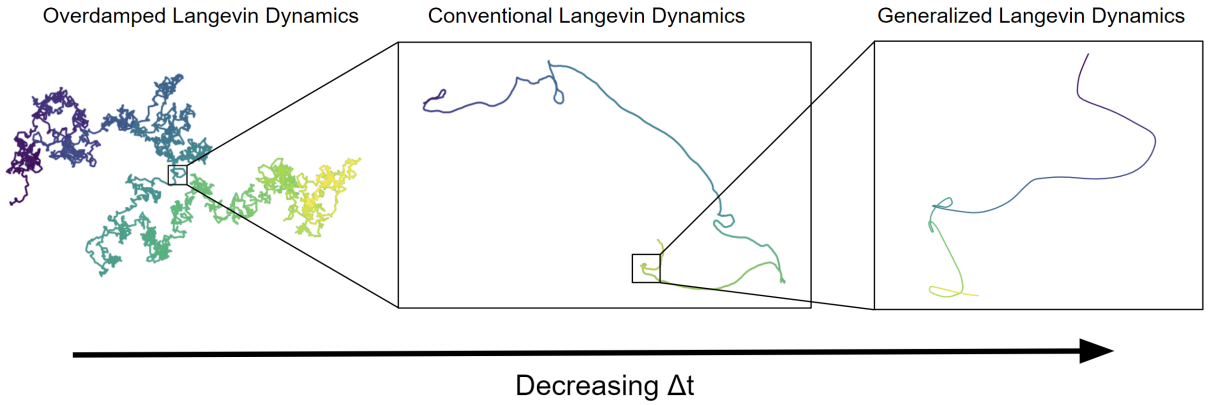

FIGURE 3.1: Self-regulated coarse-graining; how time step reduces the effective model

are written using a full step Δt, while splittings use, by substitution, $\frac{\Delta t}{2}$. Further, we define $\theta_k = e^{-\nu_k \Delta t}$, $\omega^2 = \sum_{k=1}^{M} \omega_k^2$, $\mathbf{s}^n = \sum_{k=1}^{M} \omega_k \mathbf{s}_k^n / \omega$, and $\xi_k = \sqrt{(1-\theta_k^2)\frac{k_B T}{m}} \boldsymbol{\mathcal{N}}_k^n$ for a Gaussian random variable with zero mean and unit variance $\boldsymbol{\mathcal{N}}_k^n$.

The full HOURS integrator, with the described splitting and updates, is the following.

$$\mathrm{V}\left\{\mathbf{v}^{n+1/4} = \mathbf{v}^n + \frac{b\Delta t}{2m}\mathbf{f}^n \right. \tag{3.14a}$$

$$\mathrm{X}\left\{\mathbf{x}^{n+1/2} = \mathbf{x}^n + \frac{b\Delta t}{2}\mathbf{v}^{n+1/4} \right. \tag{3.14b}$$

$$\mathrm{E}\begin{cases} \mathbf{v}^{n+2/4} = \mathbf{v}^{n+1/4}\cos\left(\frac{\omega\Delta t}{2}\right) + \mathbf{s}^n \sin\left(\frac{\omega\Delta t}{2}\right) \\ \mathbf{s}_k^{n+1/3} = \mathbf{s}_k^n + \frac{\omega_k \mathbf{s}^n}{\omega}\left(\cos\left(\frac{\omega\Delta t}{2}\right) - 1\right) - \frac{\omega_k \mathbf{v}^{n+1/4}}{\omega}\sin\left(\frac{\omega\Delta t}{2}\right) \end{cases} \tag{3.14c}$$

$$\mathrm{O}\left\{\mathbf{s}_k^{n+2/3} = \theta_k \mathbf{s}_k^{n+1/3} + \sqrt{(1-\theta_k^2)\frac{k_B T}{m}}\boldsymbol{\mathcal{N}}_k^n \right. \tag{3.14d}$$

$$\mathrm{E}\begin{cases} \mathbf{s}_k^{n+1} = \mathbf{s}_k^{n+2/3} + \frac{\omega_k \mathbf{s}^{n+2/3}}{\omega}\left(\cos\left(\frac{\omega\Delta t}{2}\right) - 1\right) - \frac{\omega_k \mathbf{v}^{n+2/4}}{\omega}\sin\left(\frac{\omega\Delta t}{2}\right) \\ \mathbf{v}^{n+3/4} = \mathbf{v}^{n+2/4}\cos\left(\frac{\omega\Delta t}{2}\right) + \mathbf{s}^{n+2/3}\sin\left(\frac{\omega\Delta t}{2}\right) \end{cases} \tag{3.14e}$$

$$\mathrm{X}\left\{\mathbf{x}^{n+1} = \mathbf{x}^{n+1/2} + \frac{b\Delta t}{2}\mathbf{v}^{n+3/4} \right. \tag{3.14f}$$

$$\mathrm{V}\left\{\mathbf{v}^{n+1} = \mathbf{v}^{n+3/4} + \frac{b\Delta t}{2m}\mathbf{f}^{n+1} \right. \tag{3.14g}$$

having $\theta_k = e^{-\nu_k \Delta t}$, $\omega^2 = \sum_{k=1}^{M} \omega_k^2$, $\mathbf{s}^n = \sum_{k=1}^{M} \omega_k \mathbf{s}_k^n / \omega$, and $\mathbf{s}^{n+2/3} = \sum_{k=1}^{M} \omega_k \mathbf{s}_k^{n+2/3} / \omega$. All indices do not reflect the true value of the variable at fractional steps, although analysis of these variables at fractional steps may yield useful information about properties of the integrator.

An important realization is that the Ornstein-Uhlenbeck update is by nature a relaxation system, and as such, for large time step, we would expect the update to reduce to some equilibrium distribution for each auxiliary variable. We can see this numerically; indeed, for $\nu_k \Delta t \gg 1$, we have $\theta = e^{-\nu_k \Delta t} \approx 0$. Essentially, the value of the auxiliary variable is proportional to the Gaussian white noise process $\boldsymbol{\mathcal{N}}_k^n$. Because of the linear coupling between the velocity and

auxiliary variables in equation 2.23b, the cumulative effect of the auxiliary variables is that of a Gaussian white noise process. Effectively, this is now a conventional Langevin equation.

Due to this realization, we can think of the number of auxiliary variables in the relaxation limit as an interpolation between generalized Langevin dynamics and conventional Langevin dynamics, controlled continuously by the time step Δt. As shown in section 2.4, the effective reduction is a Langevin equation with collision frequency determined by $\gamma = \sum_{k=1}^{M} \frac{\omega_k^2}{\nu_k}$. This further defines an Ornstein-Uhlenbeck process in velocity with characteristic timescale γ, which, as above, effectively reduces to a white noise process when $\gamma \Delta t \gg 1$. The dynamics of a system whose velocity is a white noise process is known as Brownian dynamics or overdamped Langevin dynamics, and as shown by [14], a time step rescaling parameter in the deterministic updates to position and velocity is sufficient for obtaining the correct Brownian statistics at long times. We extend this to accommodate for the additional reduction from generalized Langevin dynamics to conventional Langevin dynamics as a function of time step, as shown in figure 3.1. As done by [14], we guarantee that this reduction occurs by correcting for long-time convergence errors produced by the algorithm for large Δt.

3.2 Determination of Rescaling Parameter

The diffusion coefficient is among the most important parameters that characterizes particles, as it describes the mobility of particles in media and is encountered in numerous equations of physics and chemistry. More importantly, it is experimentally accessible, making the diffusion coefficient a prime target for comparison between an integrator and a physical system. Indeed, an ideal integrator would be able to recover the correct diffusion coefficient regardless of the size of time step. [15] and [14] list seven desiderata of quantities such as the diffusion coefficient that a useful integrator should be able to reproduce. This list of desiderata is summarized in table 3.7, using the Stokes' drag coefficient γ.

As in [14], we find that requiring the continuous limit diffusion coefficient in the zero force case fixes an expression for time step rescaling b. In the white noise limit, as described in section 2.4, we have $\gamma = \sum_{k=1}^{M} \frac{\omega_k^2}{\nu_k}$, which we use to satisfy the desiderata. For the zero force case, the Fickian MSD in the continuous limit is $2Dt = \langle x^2(n) \rangle = \frac{2k_B T}{m\gamma} t$. As such, by requiring the MSD, we fix the diffusion coefficient, and thus, the rescaling parameter b. For a full derivation of b, see section 4.1. The form of b that satisfies this constraint is

$$b = \sqrt{\frac{2\sin^2\left(\frac{\|\vec{\omega}\|\Delta t}{2}\right)}{\|\vec{\omega}\|^2 \Delta t} \left(\sum_{k=1}^{M} \omega_k^2 \coth\left(\frac{\nu_k \Delta t}{2}\right)\right) \left(\sum_{k=1}^{M} \frac{\omega_k^2}{\nu_k}\right)^{-1}} \tag{3.15}$$

Force term	Quantity	Expression	Value
Zero ($f(n) = 0$)	MSD	$\langle x^2(n) \rangle$	$\frac{2k_BT}{m\gamma} n\Delta t$
	MSV	$\langle v^2(n) \rangle$	$\frac{k_BT}{m}$
	VACF	$\langle v(n)v(n+\Delta n) \rangle$	$\frac{k_BT}{m} e^{-\gamma \Delta n \Delta t}$
Uniform ($f(n) = c$)	Terminal Drift	$\langle x(n+1) - x(n) \rangle / \Delta t$	$\frac{f}{m\gamma}$
Linear ($f(n) = -kx$)	MSD	$\langle x^2(n) \rangle$	$\frac{k_BT}{mk}$
	MSV	$\langle v^2(n) \rangle$	$\frac{k_BT}{m}$
	Virial	$m\langle v^2(n) \rangle - k\langle x^2(n) \rangle$	0

Table 3.7: Desiderata

Chapter 4

Error Analysis and Evaluation

4.1 One Dimension Zero Force Analysis

Motivated by [14], we look to find an expression for the rescaling parameter by fixing the expected Fickian diffusion coefficient in zero force potential at long times.

Consider the case of particles in one dimension with zero potential (i.e. $\forall_n \mathbf{f}(\mathbf{x}) = 0$). We write the matrix form of each update operator without the random variables in block notation as follows

$$\left\| \begin{array}{c|c} \mathbf{O} & \begin{bmatrix} 1 & & \\ & 1 & \\ & & \theta \end{bmatrix} \\ \hline \mathbf{E} & \begin{bmatrix} 1 & & \\ & P & \vec{S}^\top \\ & -\vec{S} & Q \end{bmatrix} \end{array} \middle| \begin{array}{c|c} \mathbf{V} & \begin{bmatrix} 1 & \\ & 1 \\ & & I \end{bmatrix} \\ \hline \mathbf{X} & \begin{bmatrix} 1 & \frac{1}{2}b\Delta t & \\ & 1 & \\ & & I \end{bmatrix} \end{array} \right\|$$

TABLE 4.1: Matrix form of update operators for zero potential

where

$$\vec{\omega} = \begin{bmatrix} \omega_1 \\ \omega_2 \\ \vdots \\ \omega_M \end{bmatrix}, \quad \theta = \begin{bmatrix} \theta_1 & & & \\ & \theta_2 & & \\ & & \ddots & \\ & & & \theta_M \end{bmatrix}, \quad P = \cos\left(\frac{\|\vec{\omega}\|\Delta t}{2}\right), \quad \vec{S} = \frac{\vec{\omega}}{\|\vec{\omega}\|}\sin\left(\frac{\|\vec{\omega}\|\Delta t}{2}\right) \quad (4.1)$$

and

$$Q = I + \frac{1}{\|\vec{\omega}\|^2}\left(\cos\left(\frac{\|\vec{\omega}\|\Delta t}{2}\right) - 1\right)\vec{\omega}\otimes\vec{\omega} \tag{4.2}$$

The sequential application of each of these operators in the order $VXEOEXV$ yields a full update matrix Ψ.

4.1.1 Velocity and Auxiliary Variables

The first column of each update is the standard basis vector $\mathbf{e}_1$, and as such, we know that the velocity and auxiliary variables after a full step do not depend on the position at the previous step.

With this in mind, and acknowledging that V is the identity matrix and can thus be removed without modifying the full update, consider the updates done by the application of EOE. For simplicity, we remove position from the related operators.

$$EOE = \begin{bmatrix} P & \vec{S}^\top \\ -\vec{S} & Q \end{bmatrix}\begin{bmatrix} 1 & \\ & \theta \end{bmatrix}\begin{bmatrix} P & \vec{S}^\top \\ -\vec{S} & Q \end{bmatrix} = \begin{bmatrix} P^2 - \vec{S}^\top\theta\vec{S} & P\vec{S}^\top + \vec{S}^\top\theta Q \\ -P\vec{S} - Q\theta\vec{S} & -\vec{S}\vec{S}^\top + Q\theta Q \end{bmatrix} \tag{4.3}$$

We know then that the velocity and auxiliary variables after a full update step are

$$\begin{bmatrix} \mathbf{v}^{n+1} \\ \vec{s}^{n+1} \end{bmatrix} = \begin{bmatrix} P^2 - \vec{S}^\top\theta\vec{S} & P\vec{S}^\top + \vec{S}^\top\theta Q \\ -P\vec{S} - Q\theta\vec{S} & -\vec{S}\vec{S}^\top + Q\theta Q \end{bmatrix}\begin{bmatrix} \mathbf{v}^{n} \\ \vec{s}^{n} \end{bmatrix} + \begin{bmatrix} P & \vec{S}^\top \\ -\vec{S} & Q \end{bmatrix}\vec{\xi}^n \tag{4.4}$$

where

$$\vec{s}^n = \begin{bmatrix} \mathbf{s}_1^n \\ \mathbf{s}_2^n \\ \vdots \\ \mathbf{s}_M^n \end{bmatrix} \tag{4.5}$$

and $\vec{\xi}^n$ is a vector of random variables

$$\vec{\xi}^n = \begin{bmatrix} 0 \\ \sqrt{(1-\theta_1^2)\frac{k_B T}{m}}\boldsymbol{\mathcal{N}}_1^n \\ \sqrt{(1-\theta_2^2)\frac{k_B T}{m}}\boldsymbol{\mathcal{N}}_2^n \\ \vdots \\ \sqrt{(1-\theta_M^2)\frac{k_B T}{m}}\boldsymbol{\mathcal{N}}_M^n \end{bmatrix} \tag{4.6}$$

4.1.1.1 Useful Properties of Update Matrices

Consider the product $EE^\top$.

$$EE^\top = \begin{bmatrix} P & \vec{S}^\top \\ -\vec{S} & Q \end{bmatrix} \begin{bmatrix} P & -\vec{S}^\top \\ \vec{S} & Q^\top \end{bmatrix} = \begin{bmatrix} P^2 + \vec{S}\cdot\vec{S} & -P\vec{S}^\top + \vec{S}^\top Q^\top \\ -P\vec{S} + Q\vec{S} & \vec{S}\vec{S}^\top + QQ^\top \end{bmatrix} \tag{4.7}$$

Note that

$$P^2 + \vec{S}\cdot\vec{S} = \cos^2\left(\frac{\|\vec{\omega}\|\Delta t}{2}\right) + \sin^2\left(\frac{\|\vec{\omega}\|\Delta t}{2}\right) = 1 \tag{4.8}$$

Next, consider the product $Q\vec{S}$

$$\begin{aligned} Q\vec{S} &= \vec{S} + \frac{1}{\|\vec{\omega}\|^2}\left(\cos\left(\frac{\|\vec{\omega}\|\Delta t}{2}\right) - 1\right)\vec{\omega}\otimes\vec{\omega}\vec{S} && (4.9a)\\ &= \vec{S} + \frac{1}{\|\vec{\omega}\|^3}\left(\cos\left(\frac{\|\vec{\omega}\|\Delta t}{2}\right) - 1\right)\vec{\omega}\vec{\omega}^\top\vec{\omega}\sin\left(\frac{\|\vec{\omega}\|\Delta t}{2}\right) && (4.9b)\\ &= \vec{S} + \frac{\vec{\omega}}{\|\vec{\omega}\|}\left(\cos\left(\frac{\|\vec{\omega}\|\Delta t}{2}\right) - 1\right)\sin\left(\frac{\|\vec{\omega}\|\Delta t}{2}\right) && (4.9c)\\ &= \vec{S}\cos\left(\frac{\|\vec{\omega}\|\Delta t}{2}\right) && (4.9d)\\ &= P\vec{S} && (4.9e) \end{aligned}$$

Lastly, consider $\vec{S}\vec{S}^\top$

$$\vec{S}\vec{S}^\top = \frac{1}{\|\vec{\omega}\|^2}\sin^2\left(\frac{\|\vec{\omega}\|\Delta t}{2}\right)\vec{\omega}\otimes\vec{\omega} \tag{4.10}$$

and $QQ^\top$, noting that Q is symmetric and thus $Q^\top = Q$

$$QQ^\top = \left(I + \frac{1}{\|\vec{\omega}\|^2}\left(\cos\left(\frac{\|\vec{\omega}\|\Delta t}{2}\right) - 1\right)\vec{\omega}\otimes\vec{\omega}\right)\left(I + \frac{1}{\|\vec{\omega}\|^2}\left(\cos\left(\frac{\|\vec{\omega}\|\Delta t}{2}\right) - 1\right)\vec{\omega}\otimes\vec{\omega}\right) \tag{4.11a}$$

$$= I + \frac{2}{\|\vec{\omega}\|^2}\left(\cos\left(\frac{\|\vec{\omega}\|\Delta t}{2}\right) - 1\right)\vec{\omega}\otimes\vec{\omega} + \frac{\vec{\omega}\cdot\vec{\omega}}{\|\vec{\omega}\|^4}\left(\cos\left(\frac{\|\vec{\omega}\|\Delta t}{2}\right) - 1\right)^2\vec{\omega}\otimes\vec{\omega} \tag{4.11b}$$

$$= I + \frac{2}{\|\vec{\omega}\|^2}\left(\cos\left(\frac{\|\vec{\omega}\|\Delta t}{2}\right) - 1\right)\vec{\omega}\otimes\vec{\omega} + \frac{1}{\|\vec{\omega}\|^2}\left(1 - 2\cos\left(\frac{\|\vec{\omega}\|\Delta t}{2}\right) + \cos^2\left(\frac{\|\vec{\omega}\|\Delta t}{2}\right)\right)\vec{\omega}\otimes\vec{\omega} \tag{4.11c}$$

$$= I - \frac{1}{\|\vec{\omega}\|^2}\vec{\omega}\otimes\vec{\omega} + \frac{1}{\|\vec{\omega}\|^2}\cos^2\left(\frac{\|\vec{\omega}\|\Delta t}{2}\right)\vec{\omega}\otimes\vec{\omega} \tag{4.11d}$$

$$= I - \frac{1}{\|\vec{\omega}\|^2}\left(1 - \cos^2\left(\frac{\|\vec{\omega}\|\Delta t}{2}\right)\right)\vec{\omega}\otimes\vec{\omega} \tag{4.11e}$$

$$= I - \frac{1}{\|\vec{\omega}\|^2}\sin^2\left(\frac{\|\vec{\omega}\|\Delta t}{2}\right)\vec{\omega}\otimes\vec{\omega} \tag{4.11f}$$

$$= I - \vec{S}\vec{S}^\top \tag{4.11g}$$

It follows that $QQ^\top + \vec{S}\vec{S}^\top = I$.

If we substitute equations 4.8, 4.9 4.10, and 4.11 into 4.7, we find that

$$EE^\top = \begin{bmatrix} 1 & 0 \\ 0 & I \end{bmatrix} = I \tag{4.12}$$

As such, $E^\top = E^{-1}$, or equivalently, E must be an orthogonal matrix.

Now, consider the full update matrix $\Psi = EOE$. As E is orthogonal, all eigenvalues of E have modulus 1, and as a linear transformation, E preserves vector lengths. As such, O is the only update that modifies the vector length, and as all $\theta_k < 1$, O generally shrinks vectors. The only element of O that is 1 is the first element on the diagonal, which is necessarily 1. This means that the eigenvalues of Ψ all have modulus less than or equal to 1.

Assume $\vec{w}$ to be an eigenvector of Ψ with eigenvalue λ that has modulus 1. This means that $|\Psi\vec{w}| = |\vec{w}|$, which can only be the case, as E preserves vector lengths, when $|O(E\vec{w})| = |E\vec{w}|$. This implies that $E\vec{w} = [m\ 0\ \ldots\ 0]^\top = \vec{z}$ where m has modulus 1, as the only component of O that preserves vector lengths is the first element on the diagonal. As such, we have $EOE\vec{w} = EO\vec{z} = E\vec{z} = \lambda\vec{w} = \lambda E^\top\vec{z}$, which can only be the case when the first column of E is equal to the first row of E multiplied by a constant that has modulus 1. This is only possible in the case when $\cos\left(\frac{\|\vec{\omega}\|\Delta t}{2}\right) = 0$ or when $\sin\left(\frac{\|\vec{\omega}\|\Delta t}{2}\right) = 0$, which, for well chosen values of Δt need not be the case.

As such, for Δt satisfying $\cos\left(\frac{\|\vec{\omega}\|\Delta t}{2}\right) \neq 0$ and $\sin\left(\frac{\|\vec{\omega}\|\Delta t}{2}\right) \neq 0$, EOE has eigenvalues with modulus all less than 1, ensuring Schur stability of the full update matrix Ψ.

4.1.1.2 Expectation Value Equation

Given some state vector for the velocity and auxiliary variables

$$\vec{p}^n = \begin{bmatrix} v^n \\ \\ \vec{s}^n \end{bmatrix} \tag{4.13}$$

we know

$$\vec{p}^{n+1} = EOE\vec{p}^n + E\vec{\xi}^n \tag{4.14}$$

Consider the expectation value of its outer product with itself

$$\begin{aligned}
\left\langle \vec{p}^{n+1} \otimes \vec{p}^{n+1} \right\rangle &= \left\langle \left(EOE\vec{p}^n + E\vec{\xi}^n \right) \otimes \left(EOE\vec{p}^n + E\vec{\xi}^n \right) \right\rangle && \text{(4.15a)} \\
&= \left\langle \left(EOE\vec{p}^n + E\vec{\xi}^n \right) \left(EOE\vec{p}^n + E\vec{\xi}^n \right)^\top \right\rangle && \text{(4.15b)} \\
&= \left\langle \left(EOE\vec{p}^n + E\vec{\xi}^n \right) \left(\vec{p}^{n\top} E^\top O^\top E^\top + \vec{\xi}^{n\top} E^\top \right) \right\rangle && \text{(4.15c)} \\
&= \left\langle EOE\vec{p}^n \vec{p}^{n\top} E^\top O^\top E^\top \right\rangle + \left\langle EOE\vec{p}^n \vec{\xi}^{n\top} E^\top \right\rangle + \left\langle E\vec{\xi}^n \vec{p}^{n\top} E^\top O^\top E^\top \right\rangle + \left\langle E\vec{\xi}^n \vec{\xi}^{n\top} E^\top \right\rangle && \text{(4.15d)} \\
&= \left\langle EOE\vec{p}^n \vec{p}^{n\top} E^\top O^\top E^\top \right\rangle + \left\langle E\vec{\xi}^n \vec{\xi}^{n\top} E^\top \right\rangle && \text{(4.15e)} \\
&= EOE \left\langle \vec{p}^n \otimes \vec{p}^n \right\rangle E^\top O^\top E^\top + E \left\langle \vec{\xi}^n \otimes \vec{\xi}^n \right\rangle E^\top && \text{(4.15f)}
\end{aligned}$$

where we note that there is no correlation between random variables in $\vec{\xi}^n$ and the velocity and auxiliary variables at the beginning of the step.

Consider the final term, $E\left\langle \vec{\xi}^n \otimes \vec{\xi}^n \right\rangle E^\top$.

$$E\left\langle \vec{\xi}^n \otimes \vec{\xi}^n \right\rangle E^\top = \frac{k_B T}{m} E \begin{bmatrix} 0 & & & & \\ & 1-\theta_1^2 & & & \\ & & 1-\theta_2^2 & & \\ & & & \ddots & \\ & & & & 1-\theta_M^2 \end{bmatrix} E^\top \tag{4.16a}$$

$$= \frac{k_B T}{m} E(I - O^2)E^\top \tag{4.16b}$$

$$= \frac{k_B T}{m} I - \frac{k_B T}{m} EO^2 E^\top \tag{4.16c}$$

which is invariant to n.

We are interested in finding the long-time behavior of the algorithm, when $n \gg 1$, and would expect the algorithm to converge. Under this long-time convergence assumption, we would expect $\vec{p}^{n+1} = \vec{p}^n$. In subsection 4.1.1.3 we verify that this assumption is indeed true. For simplicity, we drop the superscript, and write the full expectation equation as

$$\langle \vec{p} \otimes \vec{p} \rangle = EOE \langle \vec{p} \otimes \vec{p} \rangle E^\top O^\top E^\top + \frac{k_B T}{m} I - \frac{k_B T}{m} EO^2 E^\top \tag{4.17}$$

4.1.1.3 Lyapunov Equation Solution

We notice that equation 4.17 is similar to a discrete-time Lyapunov equation, which can be written as

$$EOE \langle \vec{p} \otimes \vec{p} \rangle E^\top O^\top E^\top - \langle \vec{p} \otimes \vec{p} \rangle + \frac{k_B T}{m} I - \frac{k_B T}{m} EO^2 E^\top = 0 \tag{4.18}$$

The general form of the discrete-time Lyapunov equation is

$$A^\top B A - B + C = 0 \tag{4.19}$$

such that if B and C are positive-definite, then update matrix A is discrete-time stable (in a Schur stability sense). In the case that A is stable, then the solution for B is

$$B = \sum_{t=0}^{\infty} (A^\top)^t C A^t \tag{4.20}$$

where the stability condition allows the series to converge in general.

Consider the solution for equation 4.18, letting $\Psi = EOE$. As shown in subsection 4.1.1.1, for particular values of Δt, Ψ has eigenvalues with modulus all less than 1, guaranteeing that the infinite series converges.

$$\langle \vec{p} \otimes \vec{p} \rangle = \sum_{t=0}^{\infty} \Psi^t \left(\frac{k_B T}{m} I - \frac{k_B T}{m} EO^2 E^\top \right) (\Psi^\top)^t \tag{4.21a}$$

$$= \frac{k_B T}{m} \left(I - EO^2 E^\top + (EOE)(E^\top O E^\top) - (EOE)(EO^2 E^\top)(E^\top O E^\top) + \ldots \right) \tag{4.21b}$$

$$= \frac{k_B T}{m} \left(I + \sum_{t=0}^{\infty} \Psi^t \left((EOE)(E^\top O E^\top) - EO^2 E^\top \right) (\Psi^\top)^t \right) \tag{4.21c}$$

$$= \frac{k_B T}{m} \left(I + \sum_{t=0}^{\infty} \Psi^t \left(EO(EE^\top) O E^\top - EO^2 E^\top \right) (\Psi^\top)^t \right) \tag{4.21d}$$

$$= \frac{k_B T}{m} \left(I + \sum_{t=0}^{\infty} \Psi^t \left(EO^2 E^\top - EO^2 E^\top \right) (\Psi^\top)^t \right) \tag{4.21e}$$

$$= \frac{k_B T}{m} I \tag{4.21f}$$

Here, we note that, as proved in subsection 4.1.1.1, $EE^\top = I$, and $O^\top = O$ as O is diagonal. As such, alternating terms of the original series cancel out, and the series converges to $\frac{k_B T}{m} I$. Because the solution exists, the updates to the velocity and auxiliary variables must be stable.

As a result, we know that the integrator converges such that $\langle v^2 \rangle = \langle s_i^2 \rangle = \frac{k_B T}{m}$ and $\langle v s_i \rangle = \langle s_i s_j \rangle = 0$ for all $i, j \in \mathbb{Z} : i, j \in [1, M]$, such that $i \neq j$ and where M is the number of auxiliary variables.

4.1.2 Position Variables

The final update is to the position variable. The full matrix update $\Psi = XVEOEVX$ is

$$\Psi = \begin{bmatrix} 1 & \frac{1}{2} b \Delta t & \\ & 1 & \\ & & 1 \end{bmatrix} \begin{bmatrix} 1 & & \\ & P^2 - \vec{S}^\top \theta \vec{S} & P\vec{S}^\top + \vec{S}^\top \theta Q \\ & -P\vec{S} - Q\theta\vec{S} & -\vec{S}\vec{S}^\top + Q\theta Q \end{bmatrix} \begin{bmatrix} 1 & \frac{1}{2} b \Delta t & \\ & 1 & \\ & & 1 \end{bmatrix} \tag{4.22a}$$

$$= \begin{bmatrix} 1 & \frac{b\Delta t}{2} \left(1 + P^2 - \vec{S}^\top \theta \vec{S} \right) & \frac{b\Delta t}{2} \left(P\vec{S}^\top + \vec{S}^\top \theta Q \right) \\ & P^2 - \vec{S}^\top \theta \vec{S} & P\vec{S}^\top + \vec{S}^\top \theta Q \\ & -P\vec{S} - Q\theta\vec{S} & -\vec{S}\vec{S}^\top + Q\theta Q \end{bmatrix} \tag{4.22b}$$

4.1.2.1 Expectation Value Equation

Given some state vector for the position, velocity, and auxiliary variables

$$\vec{p}^n = \begin{bmatrix} x^n \\ v^n \\ \vec{s}^n \end{bmatrix} \tag{4.23}$$

we know that the state after a full update is

$$\vec{p}^{n+1} = \Psi \vec{p}^n + XE\vec{\xi}^n \tag{4.24}$$

Having evaluated the expectation values of the velocity and auxiliary variables already, the only remaining values to compute are the expectation values of position with itself (MSD), and the cross correlations of position with velocity and the auxiliary variables. However, unlike velocity and the auxiliary variables, in the zero-force case we do not expect position to be bounded, and instead expect it to grow linearly with time. This means we can not make the simplifying assumption that for $n \gg 1$, $\vec{p}^{n+1} = \vec{p}^n$. Instead, we consider the update explicitly.

$$x^{n+1} = x^n + \frac{b\Delta t}{2}\left(v^n + v^{n+1}\right) \tag{4.25a}$$

$$v^{n+1} = \left(P^2 - \vec{S}^\top \theta \vec{S}\right) v^n + \left(P\vec{S}^\top + \vec{S}^\top \theta Q\right) \vec{s}^n + \vec{S}^\top \vec{\xi}^n \tag{4.25b}$$

$$s^{n+1} = \left(-P\vec{S} - Q\theta\vec{S}\right) v^n + \left(-\vec{S}\vec{S}^\top + Q\theta Q\right) \vec{s}^n + Q\vec{\xi}^n \tag{4.25c}$$

We find that the evolution of MSD is

$$\begin{aligned} \langle x^{n+1}x^{n+1}\rangle &= \langle x^n x^n\rangle + b\Delta t\langle x^n v^n\rangle + b\Delta t\langle x^n v^{n+1}\rangle + \frac{b^2\Delta t^2}{4}\langle v^n v^n\rangle + \\ &\quad \frac{b^2\Delta t^2}{2}\langle v^n v^{n+1}\rangle + \frac{b^2\Delta t^2}{4}\langle v^{n+1}v^{n+1}\rangle \end{aligned} \tag{4.26a}$$

$$\begin{aligned} &= \langle x^n x^n\rangle + b\Delta t\langle x^n v^n\rangle + b\Delta t\langle x^n v^{n+1}\rangle + \frac{b^2\Delta t^2}{4}\frac{k_B T}{m} + \\ &\quad \frac{b^2\Delta t^2}{2}\langle v^n v^{n+1}\rangle + \frac{b^2\Delta t^2}{4}\frac{k_B T}{m} \end{aligned} \tag{4.26b}$$

having

$$\langle v^n v^{n+1}\rangle = \left\langle v^n \left(\left(P^2 - \vec{S}^\top\theta\vec{S}\right)v^n + \left(P\vec{S}^\top + \vec{S}^\top\theta Q\right)\vec{s}^n + \vec{S}^\top\vec{\xi}^n\right)\right\rangle \tag{4.27a}$$

$$= \left(P^2 - \vec{S}^\top\theta\vec{S}\right)\langle v^n v^n\rangle + \left(P\vec{S}^\top + \vec{S}^\top\theta Q\right)\langle v^n\vec{s}^n\rangle + \vec{S}^\top\langle v^n\vec{\xi}^n\rangle \tag{4.27b}$$

$$= \left(P^2 - \vec{S}^\top\theta\vec{S}\right)\langle v^n v^n\rangle \tag{4.27c}$$

$$= \left(P^2 - \vec{S}^\top\theta\vec{S}\right)\frac{k_BT}{m} \tag{4.27d}$$

$$\langle v^n s^{n+1}\rangle = (-P\vec{S} - Q\theta\vec{S})\frac{k_BT}{m} \tag{4.27e}$$

and

$$\langle x^n v^{n+1}\rangle = \left\langle x^n \left(\left(P^2 - \vec{S}^\top\theta\vec{S}\right)v^n + \left(P\vec{S}^\top + \vec{S}^\top\theta Q\right)\vec{s}^n + \vec{S}^\top\vec{\xi}^n\right)\right\rangle \tag{4.28a}$$

$$= \left(P^2 - \vec{S}^\top\theta\vec{S}\right)\langle x^n v^n\rangle + \left(P\vec{S}^\top + \vec{S}^\top\theta Q\right)\langle x^n\vec{s}^n\rangle + \vec{S}^\top\langle x^n\vec{\xi}^n\rangle \tag{4.28b}$$

$$= \left(P^2 - \vec{S}^\top\theta\vec{S}\right)\langle x^n v^n\rangle + \left(P\vec{S}^\top + \vec{S}^\top\theta Q\right)\langle x^n\vec{s}^n\rangle \tag{4.28c}$$

$$\langle x^n s^{n+1}\rangle = (-P\vec{S} - Q\theta\vec{S})\langle x^n v^n\rangle + (-\vec{S}\vec{S}^\top + Q\theta Q)\langle x^n s^n\rangle \tag{4.28d}$$

$$\langle x^{n+1} v^{n+1}\rangle = \langle x^n v^{n+1}\rangle + \frac{b\Delta t}{2}\langle v^n v^{n+1}\rangle + \frac{b\Delta t}{2}\langle v^{n+1} v^{n+1}\rangle \tag{4.28e}$$

$$\langle x^{n+1} s^{n+1}\rangle = \langle x^n s^{n+1}\rangle + \frac{b\Delta t}{2}\langle v^n s^{n+1}\rangle + \frac{b\Delta t}{2}\langle v^{n+1} s^{n+1}\rangle \tag{4.28f}$$

which results in the following recurrent system of equations

$$\langle x^{n+1}v^{n+1}\rangle = \left(P^2 - \vec{S}^\top\theta\vec{S}\right)\langle x^n v^n\rangle + \left(P\vec{S}^\top + \vec{S}^\top\theta Q\right)\langle x^n\vec{s}^n\rangle + \frac{b\Delta t}{2}\frac{k_BT}{m}\left(1 + P^2 - \vec{S}^\top\theta\vec{S}\right) \tag{4.29a}$$

$$\langle x^{n+1}\vec{s}^{n+1}\rangle = \left(-P\vec{S} - Q\theta\vec{S}\right)\langle x^n v^n\rangle + \left(-\vec{S}\vec{S}^\top + Q\theta Q\right)\langle x^n\vec{s}^n\rangle + \frac{b\Delta t}{2}\frac{k_BT}{m}\left(-P\vec{S} - Q\theta\vec{S}\right) \tag{4.29b}$$

4.1.2.2 Explicit Matrix Evaluation

We note that we can rewrite this in terms of the velocity and auxiliary variable update matrices, and as the eigenvalues of EOE all have modulus less than 1, we know that $\langle x^n v^n\rangle$ and $\langle x^n\vec{s}^n\rangle$ converge. As such, this gives, after dropping superscripts for simplicity

$$\begin{bmatrix}\langle xv\rangle \\ \langle x\vec{s}\rangle\end{bmatrix} = EOE\begin{bmatrix}\langle xv\rangle \\ \langle x\vec{s}\rangle\end{bmatrix} + \frac{b\Delta t}{2}\frac{k_BT}{m}(I + EOE)\begin{bmatrix}1 \\ 0\end{bmatrix} \tag{4.30}$$

or, equivalently,

$$(I - EOE)\begin{bmatrix}\langle xv\rangle \\ \\ \langle x\vec{s}\rangle\end{bmatrix} = \frac{b\Delta t}{2}\frac{k_B T}{m}(I + EOE)\begin{bmatrix}1 \\ \\ 0\end{bmatrix} \tag{4.31}$$

We write the vector of expectation values as $\vec{p}$, and find that

$$(I - EOE)\vec{p} = \frac{b\Delta t}{2}\frac{k_B T}{m}(I + EOE)\begin{bmatrix}1 \\ \\ 0\end{bmatrix} \tag{4.32a}$$

$$\vec{p} = \frac{b\Delta t}{2}\frac{k_B T}{m}(I - EOE)^{-1}(I + EOE)\begin{bmatrix}1 \\ \\ 0\end{bmatrix} \tag{4.32b}$$

$$= \frac{b\Delta t}{2}\frac{k_B T}{m}\left(\sum_{t=0}^{\infty}(EOE)^t\right)(I + EOE)\begin{bmatrix}1 \\ \\ 0\end{bmatrix} \tag{4.32c}$$

$$= \frac{b\Delta t}{2}\frac{k_B T}{m}\left(\sum_{t=0}^{\infty}(EOE)^t + (EOE)^{t+1}\right)\begin{bmatrix}1 \\ \\ 0\end{bmatrix} \tag{4.32d}$$

$$= \frac{b\Delta t}{2}\frac{k_B T}{m}\left(\left(\sum_{t=0}^{\infty}(EOE)^t + (EOE)^t\right) - I\right)\begin{bmatrix}1 \\ \\ 0\end{bmatrix} \tag{4.32e}$$

$$= \frac{b\Delta t}{2}\frac{k_B T}{m}\left(2\left(\sum_{t=0}^{\infty}(EOE)^t\right) - I\right)\begin{bmatrix}1 \\ \\ 0\end{bmatrix} \tag{4.32f}$$

$$= \frac{b\Delta t}{2}\frac{k_B T}{m}\left(2(I - EOE)^{-1} - I\right)\begin{bmatrix}1 \\ \\ 0\end{bmatrix} \tag{4.32g}$$

By the Woodbury matrix identity, this is equivalent to

$$\vec{p} = \frac{b\Delta t}{2}\frac{k_B T}{m}\left(\left(2(I + E(-O)E)^{-1} - I\right)\begin{bmatrix}1\\0\end{bmatrix}\right) \tag{4.33a}$$

$$= \frac{b\Delta t}{2}\frac{k_B T}{m}\left(\left(2\left(I - E(-O^{-1} + EE)^{-1}E\right) - I\right)\begin{bmatrix}1\\0\end{bmatrix}\right) \tag{4.33b}$$

$$= \frac{b\Delta t}{2}\frac{k_B T}{m}\left((I - E(-O^{-1} + EE)^{-1}E)\begin{bmatrix}1\\0\end{bmatrix}\right) \tag{4.33c}$$

$$= \frac{b\Delta t}{2}\frac{k_B T}{m}\left(\begin{bmatrix}1\\0\end{bmatrix} - E(-O^{-1} + EE)^{-1}E\begin{bmatrix}1\\0\end{bmatrix}\right) \tag{4.33d}$$

For simplicity, let $\alpha = \frac{\|\omega\|\Delta t}{2}$.

$$-O^{-1} + EE = \begin{bmatrix} P^2 - \vec{S}^\top\vec{S} - 1 & P\vec{S}^\top + \vec{S}^\top Q \\ -P\vec{S} - Q\vec{S} & -\vec{S}\vec{S}^\top + QQ - \theta^{-1}\end{bmatrix} \tag{4.34a}$$

$$= \begin{bmatrix} \cos^2(\alpha) - \sin^2(\alpha) - 1 & 2\cos(\alpha)\frac{\sin(\alpha)}{\|\omega\|}\vec{\omega}^\top \\ -2\cos(\alpha)\frac{\sin(\alpha)}{\|\omega\|}\vec{\omega} & I - 2\frac{\sin^2(\alpha)}{\|\omega\|^2}\vec{\omega}\vec{\omega}^\top - \theta^{-1}\end{bmatrix} \tag{4.34b}$$

$$= \begin{bmatrix} -2\sin^2(\alpha) & \frac{\sin(2\alpha)}{\|\omega\|}\vec{\omega}^\top \\ -\frac{\sin(2\alpha)}{\|\omega\|}\vec{\omega} & I - \theta^{-1} - 2\frac{\sin^2(\alpha)}{\|\omega\|^2}\vec{\omega}\vec{\omega}^\top\end{bmatrix} \tag{4.34c}$$

To compute the inverse $(-O^{-1} + EE)^{-1}$, we use the block matrix inverse. Given specific choice of Δt, we can guarantee that $-2\sin^2(\alpha)$ is non-zero, and thus invertible. We first find the inverse of the Schur complement of $-2\sin^2(\alpha)$ in $-O^{-1} + EE$.

$$I - \theta^{-1} - 2\frac{\sin^2(\alpha)}{\|\omega\|^2}\vec{\omega}\vec{\omega}^\top - \left(-\frac{\sin(2\alpha)}{\|\omega\|}\vec{\omega}\right)\left(\frac{1}{-2\sin^2(\alpha)}\right)\left(\frac{\sin(2\alpha)}{\|\omega\|}\vec{\omega}^\top\right) \tag{4.35a}$$

$$= I - \theta^{-1} - 2\frac{\sin^2(\alpha)}{\|\omega\|^2}\vec{\omega}\vec{\omega}^\top - \frac{\sin^2(2\alpha)}{2\sin^2(\alpha)\|\omega\|^2}\vec{\omega}\vec{\omega}^\top \tag{4.35b}$$

$$= I - \theta^{-1} - \frac{2}{\|\omega\|^2}\vec{\omega}\vec{\omega}^\top \tag{4.35c}$$

Using the Sherman-Morrison formula, we know that the inverse of this is

$$(I-\theta^{-1}-\frac{2}{\|\omega\|^2}\vec{\omega}\vec{\omega}^\top)^{-1} = (I-\theta^{-1})^{-1} + \frac{2}{\|\omega\|^2}\frac{(I-\theta^{-1})^{-1}\vec{\omega}\vec{\omega}^\top(I-\theta^{-1})^{-1}}{1-\frac{2}{\|\omega\|^2}\vec{\omega}^\top(I-\theta^{-1})^{-1}\vec{\omega}} \tag{4.36a}$$

$$= (I-\theta^{-1})^{-1} + \frac{2(I-\theta^{-1})^{-1}\vec{\omega}\vec{\omega}^\top(I-\theta^{-1})^{-1}}{\|\omega\|^2-2\vec{\omega}^\top(I-\theta^{-1})^{-1}\vec{\omega}} \tag{4.36b}$$

$$= K + \frac{2K\vec{\omega}\vec{\omega}^\top K}{\|\omega\|^2-2\vec{\omega}^\top K\vec{\omega}} \tag{4.36c}$$

where we define

$$K = (I-\theta^{-1})^{-1} = \begin{bmatrix} \frac{\theta_1}{\theta_1-1} & & \\ & \frac{\theta_2}{\theta_2-1} & \\ & & \ddots \end{bmatrix} \tag{4.37}$$

and let $R = (I-\theta^{-1}-\frac{2}{\|\omega\|^2}\vec{\omega}\vec{\omega}^\top)^{-1}$. Given R, we then invert $-O^{-1}+EE$ blockwise, as

$$(-O^{-1}+EE)^{-1} = \begin{bmatrix} \frac{1}{-2\sin^2(\alpha)} - \frac{1}{4\sin^4(\alpha)}\frac{\sin^2(2\alpha)}{\|\omega\|^2}\vec{\omega}^\top R\vec{\omega} & \frac{1}{2\sin^2(\alpha)}\frac{\sin(2\alpha)}{\|\omega\|}\vec{\omega}^\top R \\ \frac{1}{-2\sin^2(\alpha)}\frac{\sin(2\alpha)}{\|\omega\|}R\vec{\omega} & R \end{bmatrix} \tag{4.38}$$

We then explicitly compute the matrix multiplication given by equation 4.33d

$$(-O^{-1}+EE)^{-1}E\begin{bmatrix}1\\0\end{bmatrix} = (-O^{-1}+EE)^{-1}\begin{bmatrix}P\\-\vec{S}\end{bmatrix} \tag{4.39a}$$

$$= \begin{bmatrix} \frac{\cos(\alpha)}{-2\sin^2(\alpha)} - \frac{\cos(\alpha)}{4\sin^4(\alpha)}\frac{\sin^2(2\alpha)}{\|\omega\|^2}\vec{\omega}^\top R\vec{\omega} - \frac{\sin(\alpha)}{2\sin^2(\alpha)}\frac{\sin(2\alpha)}{\|\omega\|^2}\vec{\omega}^\top R\vec{\omega} \\ \frac{\cos(\alpha)}{-2\sin^2(\alpha)}\frac{\sin(2\alpha)}{\|\omega\|}R\vec{\omega} - \frac{\sin(\alpha)}{\|\omega\|}R\vec{\omega} \end{bmatrix} \tag{4.39b}$$

$$= \begin{bmatrix} \frac{\cos(\alpha)}{-2\sin^2(\alpha)} - \frac{\cos(\alpha)}{\|\omega\|^2\sin^2(\alpha)}\vec{\omega}^\top R\vec{\omega} \\ -\frac{1}{\|\omega\|\sin(\alpha)}R\vec{\omega} \end{bmatrix} \tag{4.39c}$$

$$E(-O^{-1}+EE)^{-1}E\begin{bmatrix}1\\0\end{bmatrix} = \begin{bmatrix} \frac{\cos^2(\alpha)}{-2\sin^2(\alpha)} - \frac{\cos^2(\alpha)}{\|\omega\|^2\sin^2(\alpha)}\vec{\omega}^\top R\vec{\omega} - \frac{1}{\|\omega\|^2}\vec{\omega}^\top R\vec{\omega} \\ \frac{\cos(\alpha)}{2\|\omega\|\sin(\alpha)}\vec{\omega} + \frac{\cos(\alpha)}{\|\omega\|^3\sin(\alpha)}\vec{\omega}\vec{\omega}^\top R\vec{\omega} - \frac{1}{\|\omega\|\sin(\alpha)}R\vec{\omega} - \frac{\cos(\alpha)-1}{\|\omega\|^3\sin(\alpha)}\vec{\omega}\vec{\omega}^\top R\vec{\omega} \end{bmatrix} \tag{4.39d}$$

$$= \begin{bmatrix} \frac{\cos^2(\alpha)}{-2\sin^2(\alpha)} - \frac{1}{\|\omega\|^2\sin^2(\alpha)}\vec{\omega}^\top R\vec{\omega} \\ \frac{\cos(\alpha)}{2\|\omega\|\sin(\alpha)}\vec{\omega} + \frac{1}{\|\omega\|^3\sin(\alpha)}\vec{\omega}\vec{\omega}^\top R\vec{\omega} - \frac{1}{\|\omega\|\sin(\alpha)}R\vec{\omega} \end{bmatrix} \tag{4.39e}$$

which gives us

$$\begin{bmatrix}1\\0\end{bmatrix} - E(-O^{-1}+EE)^{-1}E\begin{bmatrix}1\\0\end{bmatrix} = \begin{bmatrix} 1+\frac{\cos^2(\alpha)}{2\sin^2(\alpha)}+\frac{1}{\|\omega\|^2\sin^2(\alpha)}\vec{\omega}^\top R\vec{\omega} \\ -\frac{\cos(\alpha)}{2\|\omega\|\sin(\alpha)}\vec{\omega}-\frac{1}{\|\omega\|^3\sin(\alpha)}\vec{\omega}\vec{\omega}^\top R\vec{\omega}+\frac{1}{\|\omega\|\sin(\alpha)}R\vec{\omega}\end{bmatrix} \tag{4.40a}$$

$$= \begin{bmatrix} \frac{\csc^2(\alpha)+1}{2}+\frac{1}{\|\omega\|^2\sin^2(\alpha)}\vec{\omega}^\top R\vec{\omega} \\ -\frac{\cos(\alpha)}{2\|\omega\|\sin(\alpha)}\vec{\omega}-\frac{1}{\|\omega\|^3\sin(\alpha)}\vec{\omega}\vec{\omega}^\top R\vec{\omega}+\frac{1}{\|\omega\|\sin(\alpha)}R\vec{\omega}\end{bmatrix} \tag{4.40b}$$

Consider the term $\vec{\omega}^\top R\vec{\omega}$

$$\vec{\omega}^\top R\vec{\omega} = \vec{\omega}^\top K\vec{\omega} + \frac{2\vec{\omega}^\top K\vec{\omega}\vec{\omega}^\top K\vec{\omega}}{\|\omega\|^2-2\vec{\omega}^\top K\vec{\omega}} \tag{4.41a}$$

$$= \frac{\|\omega\|^2\vec{\omega}^\top K\vec{\omega}-2\vec{\omega}^\top K\vec{\omega}\vec{\omega}^\top K\vec{\omega}}{\|\omega\|^2-2\vec{\omega}^\top K\vec{\omega}} + \frac{2\vec{\omega}^\top K\vec{\omega}\vec{\omega}^\top K\vec{\omega}}{\|\omega\|^2-2\vec{\omega}^\top K\vec{\omega}} \tag{4.41b}$$

$$= \frac{\|\omega\|^2\vec{\omega}^\top K\vec{\omega}}{\|\omega\|^2-2\vec{\omega}^\top K\vec{\omega}} \tag{4.41c}$$

$$= \frac{\|\omega\|^2\sum_k \omega_k^2\frac{\theta_k}{\theta_k-1}}{\sum_k\omega_k^2-2\omega_k^2\frac{\theta_k}{\theta_k-1}} \tag{4.41d}$$

$$= \frac{\|\omega\|^2\sum_k \omega_k^2\frac{\theta_k}{\theta_k-1}}{\sum_k\omega_k^2\frac{1+\theta_k}{1-\theta_k}} \tag{4.41e}$$

and consider the kth component of the term $R\vec{\omega}$

$$R\vec{\omega} = K\vec{\omega} + \frac{2K\vec{\omega}\vec{\omega}^\top K\vec{\omega}}{\|\omega\|^2-2\vec{\omega}^\top K\vec{\omega}} \tag{4.42a}$$

$$(R\vec{\omega})_k = -\frac{\theta_k\omega_k}{1-\theta_k} + \frac{2\omega_k\frac{\theta_k}{1-\theta_k}\left(\sum_j\omega_j^2\frac{\theta_j}{1-\theta_j}\right)}{\sum_j\omega_j^2\frac{1+\theta_j}{1-\theta_j}} \tag{4.42b}$$

$$= \frac{\omega_k\theta_k}{1-\theta_k}\left(-1+\frac{2\sum_j\omega_j^2\frac{\theta_j}{1-\theta_j}}{\sum_j\omega_j^2\frac{1+\theta_j}{1-\theta_j}}\right) \tag{4.42c}$$

$$= \frac{\omega_k\theta_k}{1-\theta_k}\left(\frac{\sum_j-\omega_j^2\frac{1+\theta_j}{1-\theta_j}+2\omega_j^2\frac{\theta_j}{1-\theta_j}}{\sum_j\omega_j^2\frac{1+\theta_j}{1-\theta_j}}\right) \tag{4.42d}$$

$$= \frac{\omega_k\theta_k}{1-\theta_k}\left(\frac{-\sum_j\omega_j^2}{\sum_j\omega_j^2\frac{1+\theta_j}{1-\theta_j}}\right) \tag{4.42e}$$

$$R\vec{\omega} = \frac{-\|\omega\|^2}{\sum_k\omega_k^2\frac{1+\theta_k}{1-\theta_k}}K\vec{\omega} \tag{4.42f}$$

which, if we substitute into equation 4.40b, yields

$$\vec{p} = \begin{bmatrix} \langle xv \rangle \\ \langle x\vec{s} \rangle \end{bmatrix} = \frac{b\Delta t}{2}\frac{k_B T}{m} \begin{bmatrix} \|\omega\|^2 \csc^2(\alpha) \left(\sum_k \omega_k^2 \frac{1+\theta_k}{1-\theta_k}\right)^{-1} \\ -\frac{\cos(\alpha)}{2\|\omega\|\sin(\alpha)}\vec{\omega} - \frac{1}{\|\omega\|\sin(\alpha)} \frac{\sum_k \omega_k^2 \frac{\theta_k}{\theta_k - 1}}{\sum_k \omega_k^2 \frac{1+\theta_k}{1-\theta_k}} \vec{\omega} - \frac{1}{\|\omega\|\sin(\alpha)} \frac{\|\omega\|^2}{\sum_k \omega_k^2 \frac{1+\theta_k}{1-\theta_k}} K\vec{\omega} \end{bmatrix} \tag{4.43}$$

4.1.2.3 Fickian MSD

Now that we know the long-time values of $\langle xv \rangle$ and $\langle x\vec{s} \rangle$, we can solve the recurrence relation for MSD, equation 4.26b. We make the additional assumption that MSD is initially 0.

$$\langle x^{n+1}x^{n+1} \rangle = \langle x^n x^n \rangle + b\Delta t \langle x^n v^n \rangle + b\Delta t \left(\left(P^2 - \vec{S}^\top \theta \vec{S} \right) \langle x^n v^n \rangle + \left(P\vec{S}^\top + \vec{S}^\top \theta Q \right) \langle x^n \vec{s}^n \rangle \right) + \frac{b^2\Delta t^2}{2}\frac{k_B T}{m} + \frac{b^2\Delta t^2}{2}\frac{k_B T}{m}\left(P^2 - \vec{S}^\top \theta \vec{S} \right) \tag{4.44a}$$

$$= \langle x^n x^n \rangle + \frac{b^2\Delta t^2}{2}\frac{k_B T}{m}\frac{2\|\omega\|^2}{\sin^2\left(\frac{\|\omega\|\Delta t}{2}\right)} \left(\sum_{k=1}^{M} \frac{\omega_k^2(1+\theta_k)}{1-\theta_k} \right)^{-1} \tag{4.44b}$$

$$\langle x^n x^n \rangle = n\frac{b^2\Delta t^2}{2}\frac{k_B T}{m}\frac{2\|\omega\|^2}{\sin^2\left(\frac{\|\omega\|\Delta t}{2}\right)} \left(\sum_{k=1}^{M} \frac{\omega_k^2(1+\theta_k)}{1-\theta_k} \right)^{-1} \tag{4.44c}$$

The expected Fickian MSD is $\frac{2tk_BT}{m\gamma} = \frac{2n\Delta t k_B T}{m\gamma}$ where we let $t = n\Delta t$, and γ is given in the white noise limit as $\sum_{k=1}^{M} \frac{\omega_k^2}{\nu_k}$. If we equate these expressions, and substitute $\theta_k = \exp(-\nu_k \Delta t)$, we can solve for an analytical expression of b as

$$b = \sqrt{\frac{2\sin^2\left(\frac{\|\vec{\omega}\|\Delta t}{2}\right)}{\|\vec{\omega}\|^2 \Delta t} \left(\sum_{k=1}^{M} \omega_k^2 \coth\left(\frac{\nu_k \Delta t}{2}\right) \right) \left(\sum_{k=1}^{M} \frac{\omega_k^2}{\nu_k} \right)^{-1}} \tag{4.45}$$

4.1.3 Zero-force Analysis Overview

Overall, the integrator with the rescaling parameter defined by equation 4.45 has the following expected values, as described in table 4.2

MSD	$\langle x^n x^n \rangle$	$\frac{2tk_BT}{m\gamma}$
MSV	$\langle v^n v^n \rangle$	$\frac{k_BT}{m}$
MS-Auxiliary	$\langle s_k^n s_k^n \rangle$	$\frac{k_BT}{m}$

TABLE 4.2: Zero-force Analysis Results

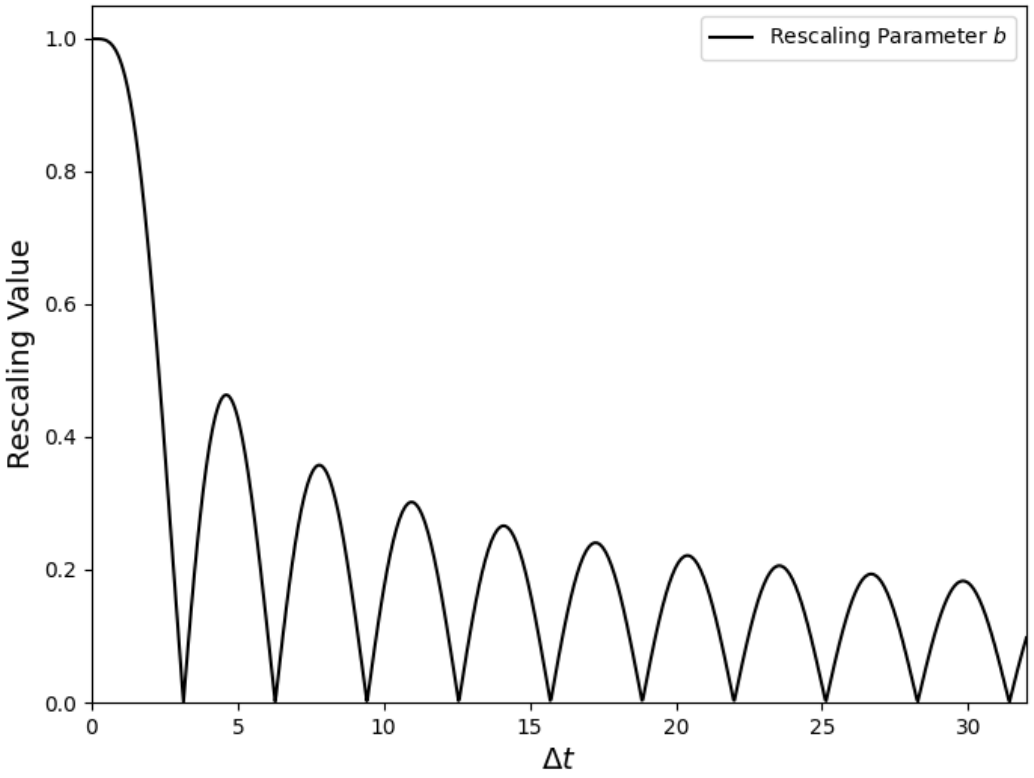

FIGURE 4.1: Rescaling parameter as a function of Δt given $\omega = \nu = 2$

4.1.4 Zero-force One Auxiliary Variable Numerical Results

To validate that these averages are recovered in practice, we performed numerical experiments to systematically compare the proposed HOURS integrator to results from literature. Consider the case of particles with a single mode ($M = 1$) and a single dimension moving in zero external potential. For simplicity, we drop the subscripts on ω_k and ν_k, and choose unit-less parameters that are order 1, having $m = k_B = T = 1$ and $\omega = \nu = 2$. With these chosen parameters, we have $\gamma = \frac{\omega^2}{\nu} = 2$. All simulations are implemented in Python.

Under these chosen parameters, the rescaling parameter has the form

$$b = \sqrt{\frac{1}{\Delta t} \sin^2(\Delta t) \coth(\Delta t)} \tag{4.46}$$

which is shown in figure 4.1. For a discussion of properties relating to the rescaling parameter, see section 4.3.

As a baseline comparison, we would expect the integrator to recover the slope of MSD at long times, as, by construction, this is what the rescaling parameter is intended to do. For

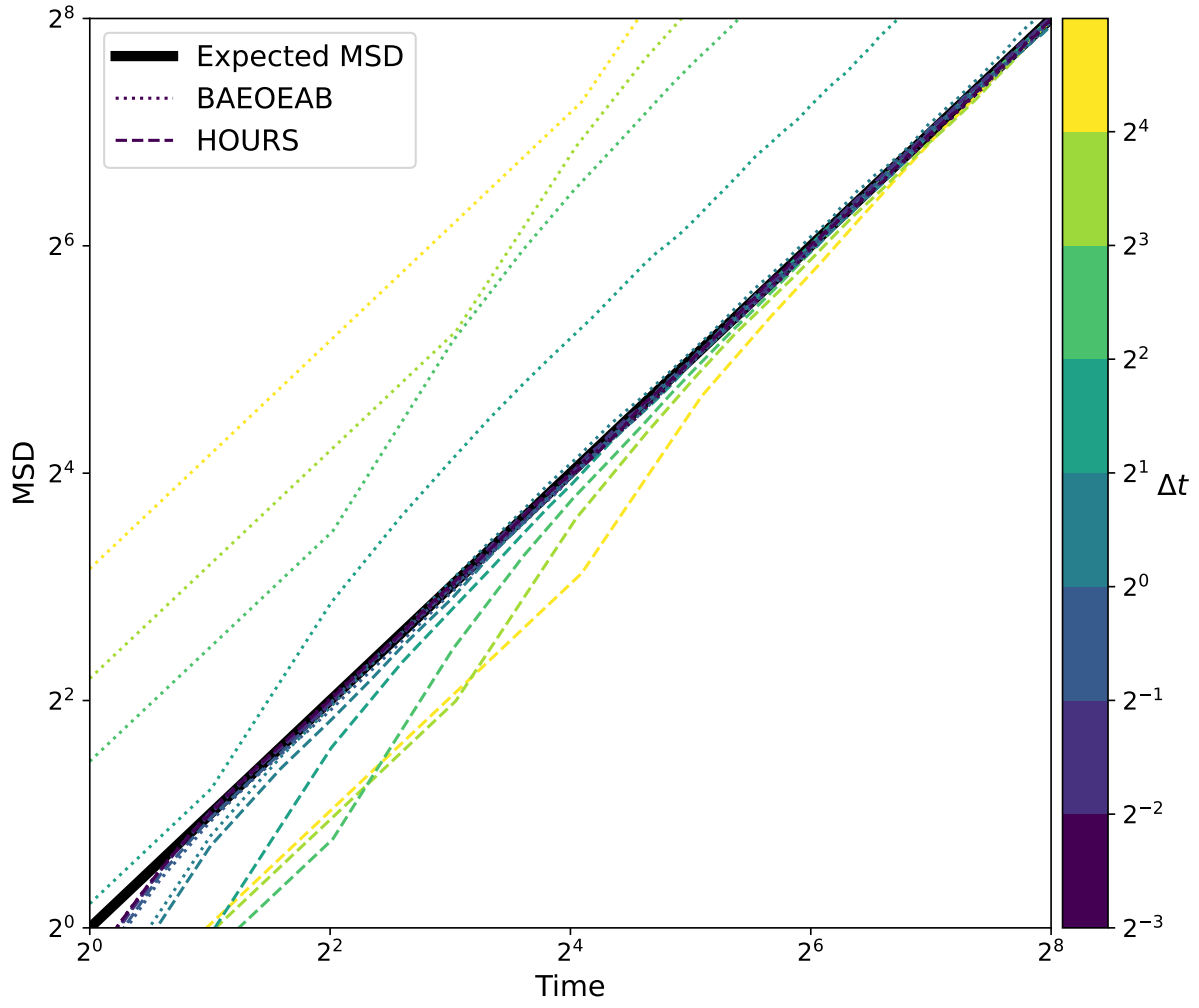

FIGURE 4.2: Log-log plot of MSD from BAEOEAB and HOURS with zero external force, one auxiliary variable, and with various Δt's

comparison, we also implement Duong and Shang's BAEOEAB integrator for the generalized Langevin equations [7]. Note that for one bath variable, the harmonic coupling update chosen by [7] is exact, and is equivalent to the exact coupling update chosen for our integrator. The only difference in implementation is we remove the effect of the rescaling parameter, setting $b = 1$.

For each simulation, we simulate 5000 particles to compute ensemble averages. Initial positions are set to 0, while auxiliary variables and velocities are initialized to the Maxwell-Boltzmann distribution, i.e. they have zero mean and variance $\frac{k_B T}{m}$. Random seeds are not fixed across simulations. We run one simulation per fixed time step, starting from $\Delta t = 2e^{-3}$ and ranging to $\Delta t = 2e^{3}$, increasing time step by powers of 2. The final time in each simulation is set to a fixed $t_F = 256$. In figure 4.2, we plot the mean squared displacement of the 5000 particles as a function of time, where the color map describes the value of Δt for the BAEOEAB integrator and for the HOURS integrator. From the figure, the HOURS integrator converges

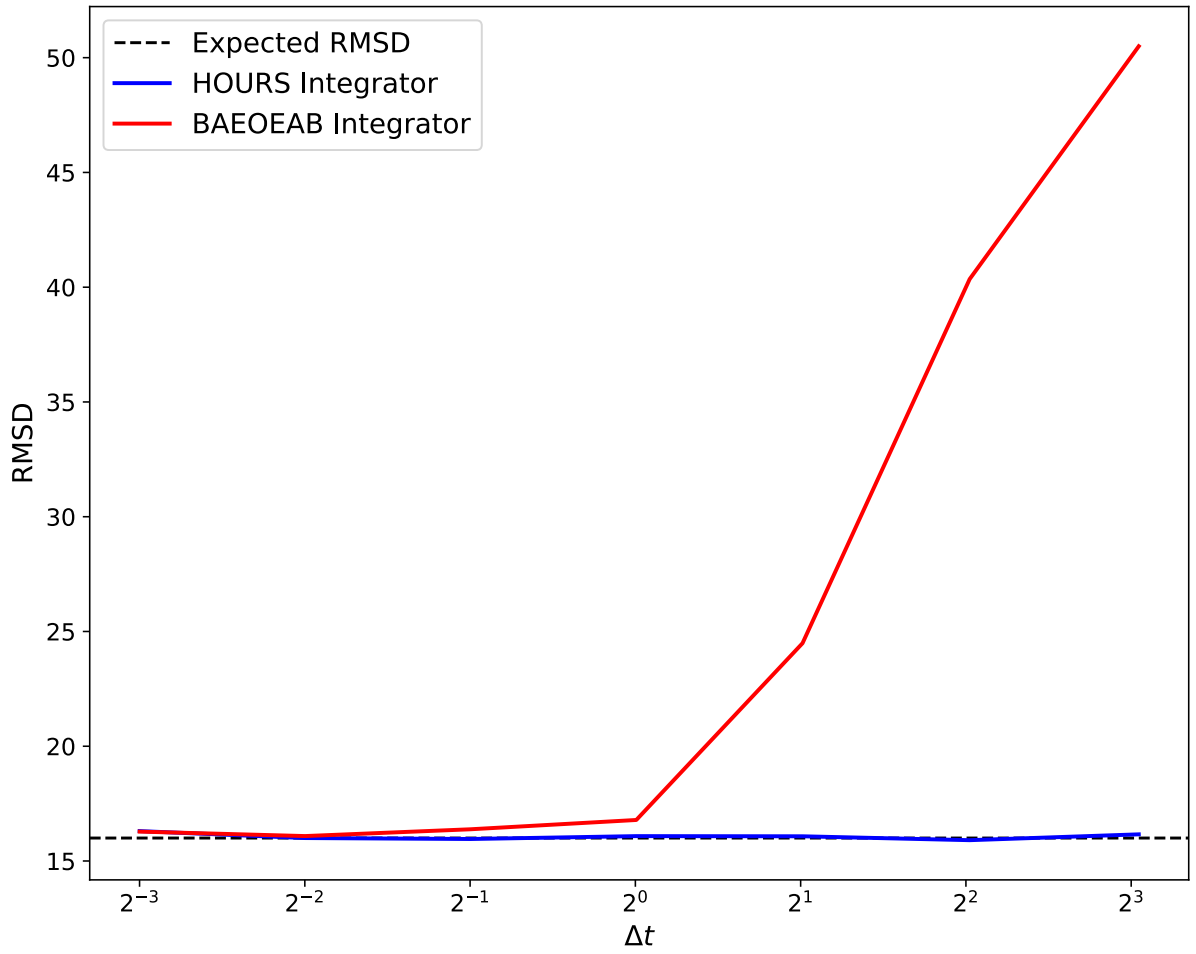

FIGURE 4.3: RMSD at $t = 256$ in zero force with a single auxiliary variable computed at various Δt's

to the expected value of MSD at long times, given by the desiderata listed in table 3.7. The BAEOEAB integrator, on the other hand, converges to a line, but as time step is increased past $\Delta t = 1$, the slope of the line increases, giving the wrong diffusion coefficient in long times.

Figure 4.3 further shows how far the BAEOEAB integrator deviates from the expected MSD for large time steps. In this plot we graph root mean square deviation (RMSD) at $t = 256$ as a function of Δt. While the HOURS integrator stays near the expected RMSD for all time steps, the error of the BAEOEAB integrator quickly grows as time step grows.

The velocity and auxiliary variable distributions for both integrators preserve their statistics for all Δt, and, as shown in figure 4.4, velocities and auxiliary variables are Boltzmann distributed across the entire simulation.

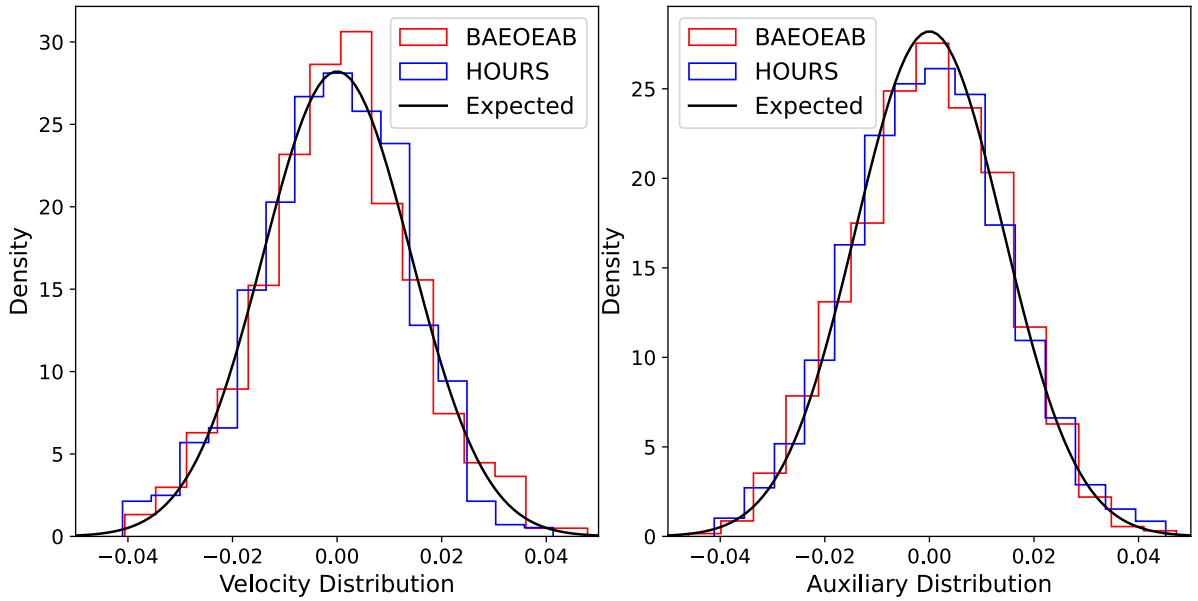

FIGURE 4.4: Histograms of the distributions of velocity and auxiliary variables across the entire simulation

4.1.5 Zero-force Two Auxiliary Variable Numerical Results

As done for the single auxiliary variable numerical experiments, we choose unit-less parameters that are order 1, having $m = k_B = T = 1$. We choose $\omega_1 = 0.5$, $\omega_2 = 0.25$, and $\nu_1 = \nu_2 = 0.15625$, which are chosen because they yield a rescaling parameter that is not close to 0 at time steps equal to powers of two, and because they yield $\gamma = 2$, as in section 4.1.4.

Under these chosen parameters, the rescaling parameter has the form as shown in figure 4.5. As opposed to the one auxiliary variable case, the BAEOEAB integrator for two auxiliary variables does not exactly solve the harmonic coupling update, which further increases error for large Δt.

For each simulation, we simulate 5000 particles to compute ensemble averages. Initial positions are set to 0, while auxiliary and velocity variables are initialized to the Maxwell-Boltzmann distribution, i.e. they have zero mean and variance $\frac{k_B T}{m}$. Random seeds are not fixed across simulations. At each time step, we run one simulation for each integrator, starting from $\Delta t = 2e^{-3}$ and ranging to $\Delta t = 2e^{4}$, increasing time step by powers of 2. The final time in each simulation is set to a fixed $t_F = 256$. In figure 4.6, we plot the mean squared displacement of the 5000 particles for each simulation as a function of time where the color map describes the value of Δt for the BAEOEAB integrator and for the HOURS integrator. From the figure, the HOURS integrator converges to the expected value of MSD at long times, given by the desiderata listed in table 3.7. Importantly, for small time steps, unique oscillatory phenomena of the generalized Langevin equations are preserved by both the BAEOEAB and

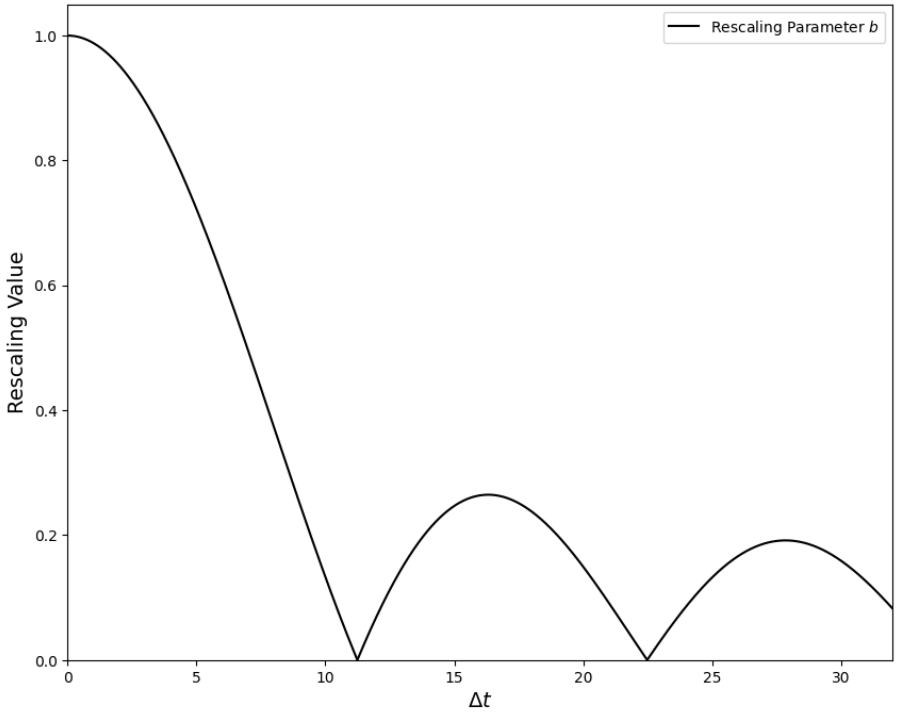

FIGURE 4.5: Rescaling parameter as a function of Δt given $\omega_1 = 0.5$, $\omega_2 = 0.25$, and $\nu_1 = \nu_2 = 0.15625$

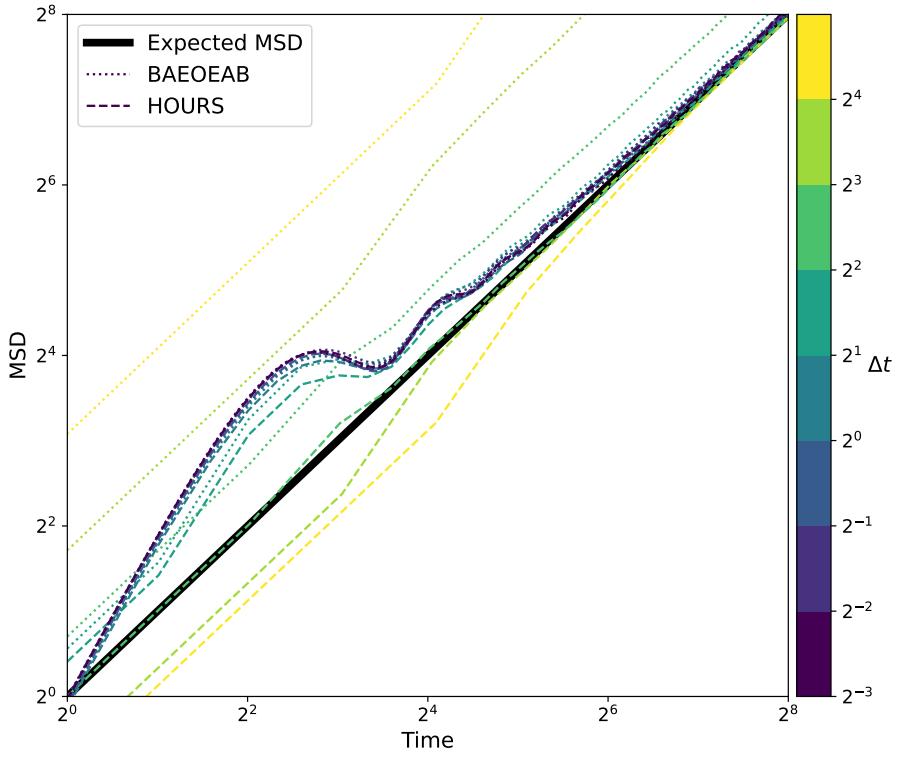

FIGURE 4.6: Log-log plot of MSD from BAEOEAB and HOURS with zero external force and two auxiliary variables with various Δt's

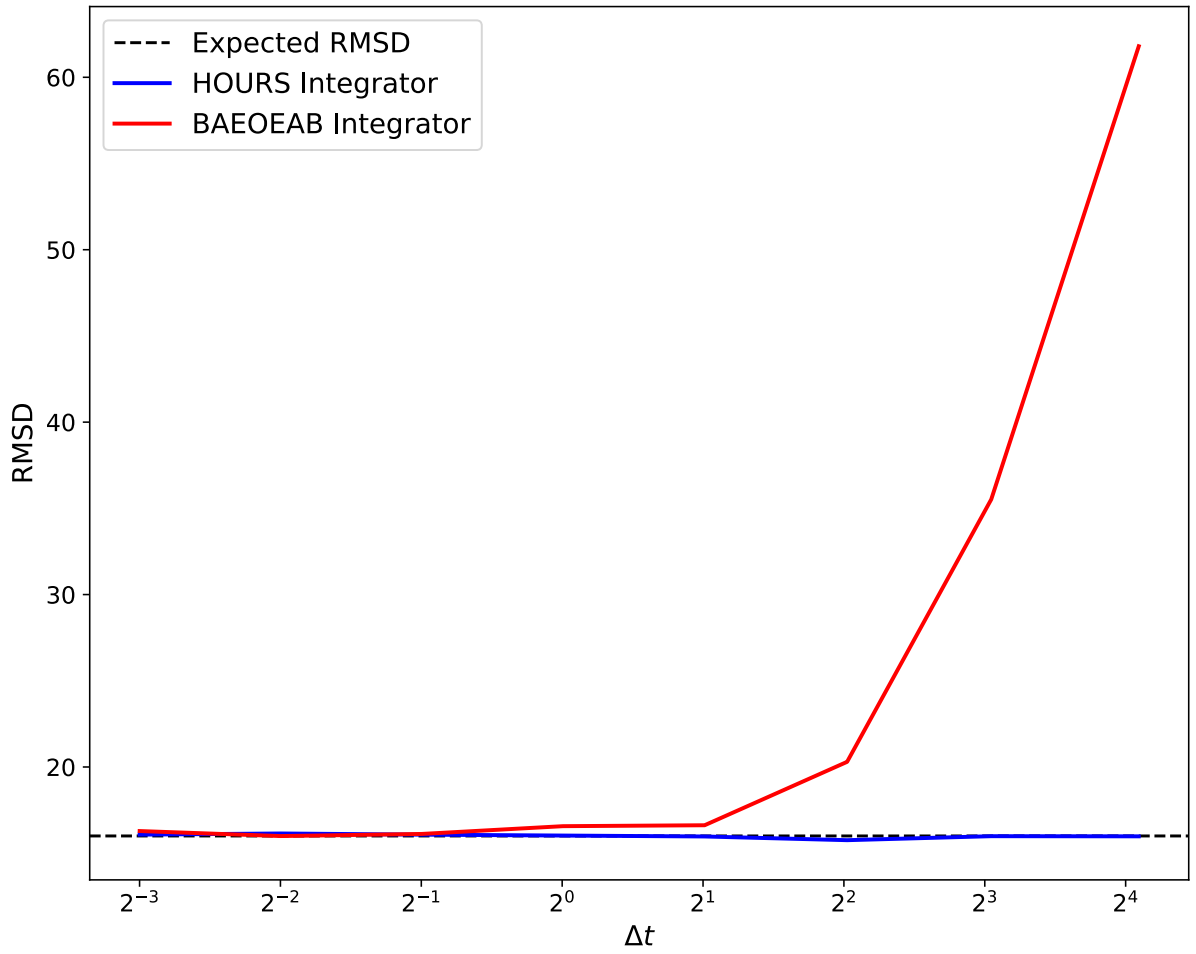

FIGURE 4.7: RMSD at $t = 256$ in zero force with two auxiliary variables computed at various Δt's

HOURS integrators. For large time steps, where this short timescale behavior is stepped over, the HOURS integrator still converges to the correct long time asymptotic behavior.

Figure 4.7 further emphasizes this result, quantifying how far the BAEOEAB integrator deviates from the expected root mean square deviation (RMSD). The plot shows the RMSD at $t = t_F = 256$, the final time in each simulation. While the HOURS integrator stays near the expected RMSD for all time steps, the error of the BAEOEAB integrator quickly grows as the time step grows.

4.2 One Dimension Harmonic Force Analysis

Consider the case of particles in one dimension with a quadratic potential (i.e. $\mathbf{f}(x) = -kx$). We write the matrix form of each update operator without the random variables in block notation in table 4.3.

$$\left\| \begin{array}{c|c} \mathbf{O} & \begin{bmatrix} 1 & & \\ & 1 & \\ & & \theta \end{bmatrix} \\ \hline \mathbf{E} & \begin{bmatrix} 1 & & \\ & P & \vec{S}^\top \\ & -\vec{S} & Q \end{bmatrix} \end{array} \middle| \begin{array}{c|c} \mathbf{V} & \begin{bmatrix} 1 & & \\ -\frac{1}{2m}kb\Delta t & 1 & \\ & & I \end{bmatrix} \\ \hline \mathbf{X} & \begin{bmatrix} 1 & \frac{1}{2}b\Delta t & \\ & 1 & \\ & & I \end{bmatrix} \end{array} \right\|$$

TABLE 4.3: Matrix form of update operators for quadratic potential

Unlike the one dimension zero force analysis conducted in section 4.1, the velocity and auxiliary variables cannot be considered a separate subsystem than the position variables due to the external force term in the deterministic velocity update V. However, we expect all variables to converge to constants, and as such, can make relevant simplifications in the expectation value equations.

In the case of one auxiliary variable, the HOURS integrator reduces exactly to BAEOEAB, and as such, in the case of a harmonic force, has the exact same expectation values at long times. Following [7] for one auxiliary variable, this gives MSD of $\frac{k_BT}{mk}$, an MSV of $\frac{k_BT}{m}\left(1-\frac{b^2\Delta t^2 k}{4m}\right)$, and a mean squared auxiliary variable of $\frac{k_BT}{m}$, with all cross correlations being 0.

4.3 Properties of the Rescaling Parameter

Recall the rescaling parameter b given from equation 4.45

$$b = \sqrt{\frac{2\sin^2\left(\frac{\|\vec{\omega}\|\Delta t}{2}\right)}{\|\vec{\omega}\|^2\Delta t}\left(\sum_{k=1}^{M}\omega_k^2\coth\left(\frac{\nu_k\Delta t}{2}\right)\right)\left(\sum_{k=1}^{M}\frac{\omega_k^2}{\nu_k}\right)^{-1}} \tag{4.47}$$

The rescaling parameter is generally well-behaved as a function of Δt. Importantly, in the limit as Δt approaches 0, b approaches 1 for all choices of ω_k and ν_k, which corresponds to standard integrators from literature in the continuous limit. This can be determined simply by L'Hôpital's rule. Note, however, that the rescaling parameter is not necessarily less than or equal to 1 for all values of ω_k and ν_k. Sometimes, the rescaling parameter may be larger than 1. Even in these cases, where b slightly boosts the time step, the zero force diffusion coefficient is preserved at long times.

Further, the analysis in section 4.1 has the conditions that $\cos\left(\frac{\|\omega\|\Delta t}{2}\right)$ and $\sin\left(\frac{\|\omega\|\Delta t}{2}\right)$ are non-zero, but the form of the derived rescaling parameter seems to only have ill-behavior when $\sin\left(\frac{\|\omega\|\Delta t}{2}\right) = 0$, as, generally, under this condition the rescaling parameter gives $b = 0$.

When $\cos\left(\frac{\|\omega\|\Delta t}{2}\right) = 0$, the rescaling parameter is near local maxima, and empirically does not seem to yield poor behavior.

The rescaling parameter scales asymptotically as $\frac{1}{\sqrt{t}}$, and as such, by choosing local maxima in b, can be used to improve computational efficiency of simulations. Indeed, the effective time step for large Δt in the position and force updates approaches $\sqrt{\Delta t}$.

Chapter 5

Conclusion and Future Work

In this thesis, we have introduced two modifications to existing integrators for the generalized Langevin equations. First, we extend a splitting method proposed by [7] to exactly solve for the coupling terms between velocity and the auxiliary bath variables. Second, we propose a time step rescaling parameter b that allows nearly any time step to be chosen while still resolving the long time statistics of the generalized Langevin equations by relaxing to the correct solution.

In this thesis, we have introduced two slight modifications to existing integrators for the generalized Langevin equations. First, we extend a splitting method proposed by [7] to exactly solve for the coupling terms between velocity and the auxiliary bath variables. Second, we propose a time step rescaling parameter b that allows nearly any time step to be chosen while still resolving the long time statistics of the generalized Langevin equations by relaxing to the correct solution. We have shown that the proposed integrator recovers the expected long-time statistics of the generalized Langevin equations in the white noise limit, and that the rescaling parameter is well-behaved for most time steps, excluding discontinuities at periodic intervals. In particular, it exactly converges to the correct mean squared velocity and mean squared bath variables.

For future work, further investigation of the behavior of the exact harmonic solve is necessary, as well as identifying properties of the rescaling parameters for practical use in molecular dynamics simulations or in path sampling contexts. This calls for a more rigorous analysis of the HOURS integrator for 2 or more auxiliary variables, and its applications to more complex potentials and higher dimensions.

An important direction for future work is to extend the idea of integration by stochastic relaxation to investigate other relaxation-type equations. This includes, but is not limited to, magneto-hydrodynamics [24], and the Basset-Boussinesq-Oseen (BBO) equation [22]. The BBO equation, in particular, is a convolution over the past velocities, which is a history effect that

has been shown to be representable by a Prony series [22, 23], which closely aligns with the memory kernel investigated in this work.

In this work, we have investigated corrections to long time dynamics. However, we have no guarantee of recovering short time or intermediate time dynamics, for arbitrary choice of time step. Preliminary results, such as those in figure 4.6, seem to suggest that intermediate time dynamics are recovered with reasonable damping for arbitrary choice of time step. Further investigation of this intermediate timescale behavior, and the investigation of predictor-corrector type integrators that address this behavior, is left to future work.

Appendix A

Overview of Ornstein-Uhlenbeck Processes

An Ornstein-Uhlenbeck process is a stochastic process originally used to describe the Langevin equation, proposed by Ornstein and Uhlenbeck in a 1930 paper titled "On the Theory of Brownian Motion" [25]. Its use evolved over time to be applied to financial mathematics and other stochastic differential equations (SDEs).

A.1 Wiener Processes

A Wiener process is a continuous-time stochastic process that is often referred to simply as Brownian motion. Any Wiener process W_t, indexed by nonnegative real numbers t, satisfies the following four properties.

1. $W_0 = 0$
2. W is continuous, i.e. W_t is continuous in t
3. Random variables defined by disjoint increments are independent; i.e. $W_{t+u} - W_t$ is independent of $W_s - W_{s-r}$ for positive coefficients u and r where $s < t$
4. Increments are Gaussian, i.e. $W_{t+u} - W_t$ is normally distributed with mean 0 and variance u

A more general kind of stochastic process is the Lévy process, which has stationary and independent increments that are not necessarily Gaussian.

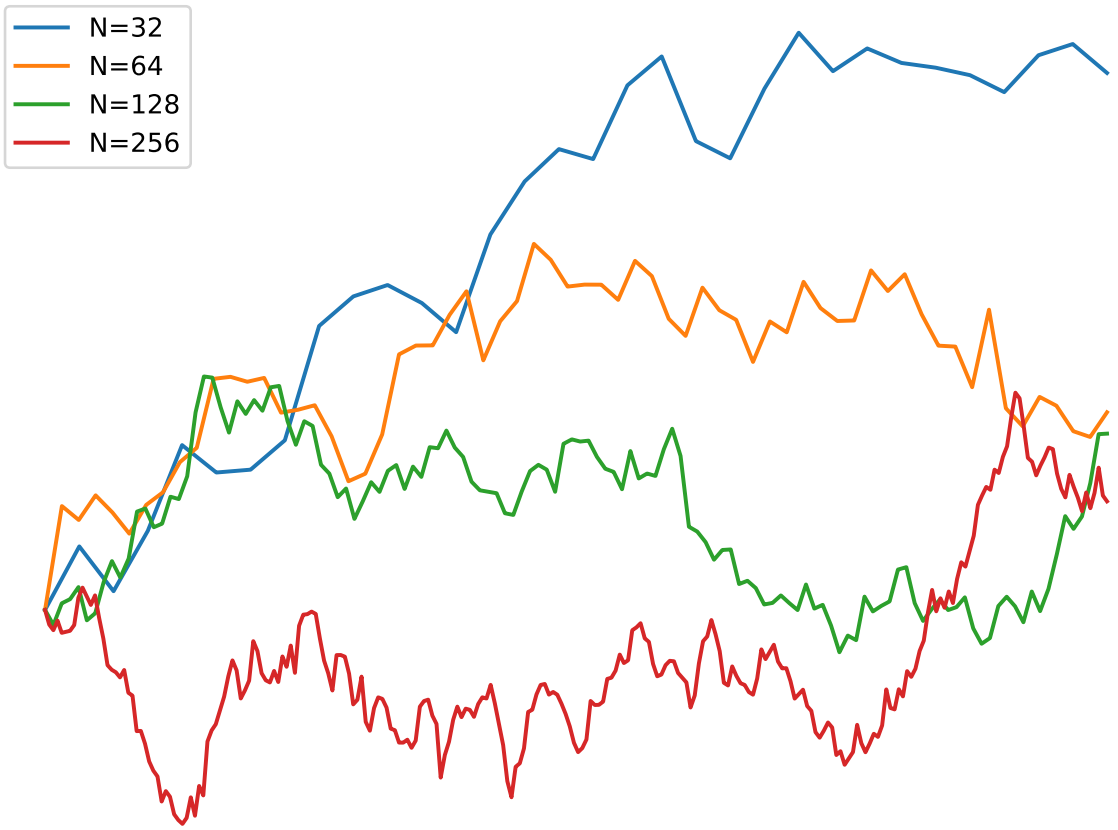

FIGURE A.1: Wiener process at different levels of spatial discretization

Intuitively, such a process can be thought of as the limit of random walks. Consider a discrete and infinite series of independent and identically distributed (i.i.d.) random variables $\mathcal{N}_i$ that have mean 0 and unit variance. For each $n \geq 1$, we can define a continuous-time stochastic process $W_n(t)$ as

$$W_n(t) = \frac{1}{\sqrt{n}} \sum_{i=1}^{\lfloor nt \rfloor} \mathcal{N}_i \tag{A.1}$$

which describes a random step function that has jumps scaled at size $\pm\frac{1}{\sqrt{n}}$, where, by the central limit, each interval $W_n(t+u) - W_n(t)$ is close to the a normal distribution with mean 0 and variance u. Indeed, in the limit as $n \to \infty$, this continuous-time process approaches a Wiener process.

As shown in figure A.1, Wiener processes are characterized by producing the same statistics over intervals independent of spatial resolution. As a consequence, many important properties of dynamic systems that have Wiener processes are independent of sampling density. It is important to remember that despite the fractal-like behavior of samplings from Wiener processes, a Wiener process is still continuous.

A.2 Ornstein-Uhlenbeck Processes

Using notation from Itô calculus, an Ornstein-Uhlenbeck (OU) process x_t is defined by the following SDE

$$dx_t = -\theta x_t dt + \sigma dW_t \tag{A.2}$$

where $\theta > 0$ and $\sigma > 0$ are parameters of the differential equation, and W_t is a Wiener process as described in section A.1. Here, if we consider x_t to describe the velocity of a particle, θ describes the average tendency of the velocity to return to equilibrium, and σ describes the magnitude of perturbation by a standard Wiener process. More realistically, when there are external forces or there exists an external potential, the velocity experiences a mean drift, which can be characterized by a natural extension to the OU process as

$$dx_t = \theta(\mu - x_t)dt + \sigma dW_t \tag{A.3}$$

having a constant μ characterize the drift. Written in standard notation, the Ornstein-Uhlenbeck process is equivalent to a Langevin equation in the form

$$\frac{dx_t}{dt} = -\theta x_t + \sigma\eta(t) \tag{A.4}$$

where $\eta(t)$ is a white noise process that replaces the derivative $\frac{dW_t}{dt}$, which does not exist as the Wiener process is nowhere differentiable [26]. Instead, we take advantage of the fact that the Wiener process has intervals that are Gaussian distributed with zero mean and variance equal to the change in time along the interval.

A.2.1 Exact Solution

The exact solution of an Ornstein-Uhlenbeck process, as it is a first-order differential equation, can be computed using methods such as variation of parameters [27]. This gives the exact solution as

$$x_t = x_0 e^{-\theta t} + \mu\left(1 - e^{-\theta t}\right) + \sigma \int_0^t e^{-\theta(t-s)} dW_s \tag{A.5}$$

which has mean

$$\mathrm{E}[x_t] = x_0 e^{-\theta t} + \mu\left(1 - e^{-\theta t}\right) \tag{A.6}$$

and covariance given by the Itô isometry

$$\mathrm{cov}[x_s, x_t] = \frac{\sigma^2}{2\theta}\left(e^{-\theta|t-s|} - e^{-\theta(t+s)}\right) \tag{A.7}$$

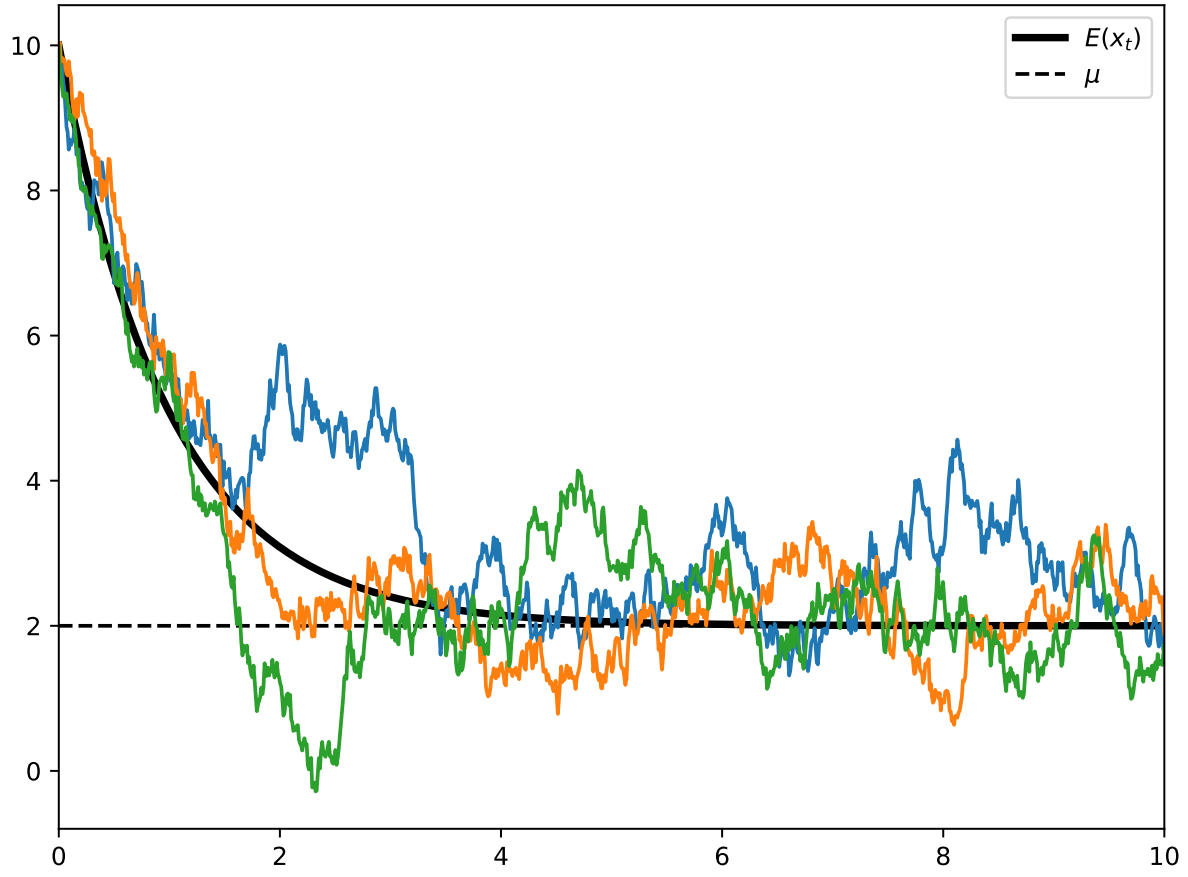

FIGURE A.2: Three simulated Ornstein-Uhlenbeck processes having $\theta = 1$, $\mu = 2$, and $\sigma = \sqrt{2}$ and the expected value of the solution

It follows then, as the Itô integral of a deterministic integrand is normally distributed, that

$$x_t = x_0 e^{-\theta t} + \mu\left(1 - e^{-\theta t}\right) + \frac{\sigma}{\sqrt{2\theta}} W_{1-e^{-2\theta t}} \tag{A.8}$$

For example, in figure A.2, we show the expected value of the solution along with 3 simulations of Ornstein-Uhlenbeck processes, having $\theta = 1$, $\mu = 2$, and $\sigma = \sqrt{2}$. Notably, as θt grows large, $e^{-\theta t}$ becomes arbitrarily small, and the process converges to a white noise process centered around μ.

Appendix B

Overview of Strang Splitting Methods

Strang splitting is a numerical method for solving linearly decomposable differential equations, first introduced by Strang in 1968 [28]. The idea of operator splitting is to reduce the complexity required in handling the sums of n differential operators into some aggregate of n solutions for each differential operator. Ultimately, this simplifies the process of obtaining a solution for the original differential equation, as long as each splitting can be solved simply.

As a motivating example, first consider an ODE in the form

$$\dot{x} = \mathcal{L}_1(x) + \mathcal{L}_2(x) \tag{B.1}$$

where x can be scalar or vector valued, and $\mathcal{L}_1$ and $\mathcal{L}_2$ are differential operators, or in the case of physical systems, sometimes termed the Liouville operator or Liouvillian [9]. If $\mathcal{L}_1$ and $\mathcal{L}_2$ are constant coefficient matrices, then the exact solution is

$$x(t) = e^{(\mathcal{L}_1+\mathcal{L}_2)t}x_0 \tag{B.2}$$

If $\mathcal{L}_1$ and $\mathcal{L}_2$ commute, then this solution can naturally be split as $e^{\mathcal{L}_1 t}e^{\mathcal{L}_2 t}$. If they do not commute, then by the Baker-Campbell-Hausdorff formula, the cost of such a split comes at second order error

$$e^{(\mathcal{L}_1+\mathcal{L}_2)t} = e^{\mathcal{L}_1 t}e^{\mathcal{L}_2 t} + O(t^2) \tag{B.3}$$

which has $O(\Delta t)$ accuracy when applied as a numerical scheme, replacing t with Δt. Instead, Strang proposed a splitting by half-step, which can be proved to be second order by Taylor expansion.

$$x(t) \approx e^{\mathcal{L}_1 \frac{\Delta t}{2}}e^{\mathcal{L}_2 \Delta t}e^{\mathcal{L}_1 \frac{\Delta t}{2}} \tag{B.4}$$

This splitting naturally extends to arbitrary numbers of differential operators $\mathcal{L}_k$, and produces a technique that is generalizable to any number of dimensions as well.

Bibliography

[1] Paolo Mereghetti, Daria Kokh, J Andrew McCammon, and Rebecca C Wade. Diffusion and association processes in biological systems: theory, computation and experiment. *BMC Biophysics*, 4(2), 03 2011. doi: 10.1186/2046-1682-4-2. URL https://doi.org/10.1186/2046-1682-4-2.

[2] D. E. Smith and C. B. Harris. Generalized Brownian dynamics. I. Numerical integration of the generalized Langevin equation through autoregressive modeling of the memory function. *The Journal of Chemical Physics*, 92(2):1304–1311, 01 1990. ISSN 0021-9606. doi: 10.1063/1.458140. URL https://doi.org/10.1063/1.458140.

[3] E. Guàrdia and J. A. Padró. Generalized Langevin dynamics simulation of interacting particles. *The Journal of Chemical Physics*, 83(4):1917–1920, 08 1985. ISSN 0021-9606. doi: 10.1063/1.449379. URL https://doi.org/10.1063/1.449379.

[4] M. Berkowitz, J. D. Morgan, and J. Andrew McCammon. Generalized Langevin dynamics simulations with arbitrary time-dependent memory kernels. *The Journal of Chemical Physics*, 78(6):3256–3261, 03 1983. ISSN 0021-9606. doi: 10.1063/1.445244. URL https://doi.org/10.1063/1.445244.

[5] Igor Goychuk and Thorsten Pöschel. Hydrodynamic memory can boost enormously driven nonlinear diffusion and transport. *Phys. Rev. E*, 102:012139, Jul 2020. doi: 10.1103/PhysRevE.102.012139. URL https://link.aps.org/doi/10.1103/PhysRevE.102.012139.

[6] Andrew D Baczewski and Stephen D Bond. Numerical integration of the extended variable generalized langevin equation with a positive prony representable memory kernel. *The Journal of chemical physics*, 139(4), 2013.

[7] Manh Hong Duong and Xiaocheng Shang. Accurate and robust splitting methods for the generalized langevin equation with a positive prony series memory kernel. *Journal of Computational Physics*, 464:111332, 2022.

[8] Hazime Mori. Transport, Collective Motion, and Brownian Motion. *Progress of Theoretical Physics*, 33(3):423–455, 03 1965. ISSN 0033-068X. doi: 10.1143/PTP.33.423. URL https://doi.org/10.1143/PTP.33.423.

[9] Robert Zwanzig. *Nonequilibrium statistical mechanics*. Oxford university press, 2001.

[10] W.F. van Gunsteren and H.J.C. Berendsen. Algorithms for brownian dynamics. *Molecular Physics*, 45(3):637–647, 1982. doi: 10.1080/00268978200100491. URL https://doi.org/10.1080/00268978200100491.

[11] W. F. Van Gunsteren and H. J. C. Berendsen. A leap-frog algorithm for stochastic dynamics. *Molecular Simulation*, 1(3):173–185, 1988. doi: 10.1080/08927028808080941. URL https://doi.org/10.1080/08927028808080941.

[12] Andrei Medved, Riley Davis, and Paula A. Vasquez. Understanding fluid dynamics from langevin and fokker–planck equations. *Fluids*, 5(1), 2020. ISSN 2311-5521. doi: 10.3390/fluids5010040. URL https://www.mdpi.com/2311-5521/5/1/40.

[13] Peter Kloeden and Eckhard Platen. *Numerical Solution of Stochastic Differential Equations*. Springer, 1992.

[14] David A Sivak, John D Chodera, and Gavin E Crooks. Time step rescaling recovers continuous-time dynamical properties for discrete-time langevin integration of nonequilibrium systems. *The Journal of Physical Chemistry B*, 118(24):6466–6474, 2014.

[15] Bernard R. Brooks Richard W. Pastor and Attila Szabo. An analysis of the accuracy of langevin and molecular dynamics algorithms. *Molecular Physics*, 65(6):1409–1419, 1988. doi: 10.1080/00268978800101881. URL https://doi.org/10.1080/00268978800101881.

[16] John Fricks, Lingxing Yao, Timothy C. Elston, and M. Gregory Forest. Time-domain methods for diffusive transport in soft matter. *SIAM Journal on Applied Mathematics*, 69 (5):1277–1308, 2009. ISSN 00361399. URL http://www.jstor.org/stable/27798732.

[17] Nathan Glatt-Holtz, David Herzog, Scott McKinley, and Hung Nguyen. The generalized langevin equation with a power-law memory in a nonlinear potential well, 2020.

[18] Raz Kupferman. Fractional kinetics in kac–zwanzig heat bath models. *Journal of Statistical Physics*, 114:291–326, 2004. URL https://api.semanticscholar.org/CorpusID:53581364.

[19] P. Siegle, I. Goychuk, and P. Hänggi. Markovian embedding of fractional superdiffusion. *EPL (Europhysics Letters)*, 93(2):20002, January 2011. ISSN 1286-4854. doi: 10.1209/0295-5075/93/20002. URL http://dx.doi.org/10.1209/0295-5075/93/20002.

[20] M. P. Allen. Configurational temperature in membrane simulations using dissipative particle dynamics. *Journal of Physical Chemistry B*, 110(8):3823—-3830, 2006. ISSN 1520-6106.

[21] M Ottobre and G A Pavliotis. Asymptotic analysis for the generalized langevin equation. *Nonlinearity*, 24(5):1629–1653, April 2011. ISSN 1361-6544. doi: 10.1088/0951-7715/24/5/013. URL http://dx.doi.org/10.1088/0951-7715/24/5/013.

[22] Igor Goychuk. Fractional hydrodynamic memory and superdiffusion in tilted washboard potentials. *Physical review letters*, 123(18):180603, 2019.

[23] Igor Goychuk. *Viscoelastic Subdiffusion: Generalized Langevin Equation Approach*, pages 187–253. John Wiley & Sons, Ltd, 2012. ISBN 9781118197714. doi: https://doi.org/10.1002/9781118197714.ch5. URL https://onlinelibrary.wiley.com/doi/abs/10.1002/9781118197714.ch5.

[24] C. E. Seyler and M. R. Martin. Relaxation model for extended magnetohydrodynamics: Comparison to magnetohydrodynamics for dense Z-pinches. *Physics of Plasmas*, 18(1):012703, 01 2011. ISSN 1070-664X. doi: 10.1063/1.3543799. URL https://doi.org/10.1063/1.3543799.

[25] G. E. Uhlenbeck and L. S. Ornstein. On the theory of the brownian motion. *Phys. Rev.*, 36:823–841, Sep 1930. doi: 10.1103/PhysRev.36.823. URL https://link.aps.org/doi/10.1103/PhysRev.36.823.

[26] Gregory Lawler. *Introduction to Stochastic Processes*. Chapman & Hall, 2006.

[27] Crispin Gardiner. *Handbook of Stochastic Methods for Physics, Chemistry, and the Natural Sciences*. Springer-Verlag, 1985.

[28] Gilbert Strang. On the construction and comparison of difference schemes. *SIAM Journal on Numerical Analysis*, 5(3):506–517, 1968. doi: 10.1137/0705041. URL https://doi.org/10.1137/0705041.